

Human Sputum Microbiome Composition and Sputum Inflammatory Cell Profiles Are Altered with Controlled Wood Smoke Exposure as a Model for Wildfire Smoke

Catalina Cobos-Uribe, MS¹ - <https://orcid.org/0000-0002-6671-0780>, Radhika Dhingra, PhD² - [http://orcid.org/0000-0003-0202-1860](https://orcid.org/0000-0003-0202-1860), Martha A. Almond^{3,4}, Neil E. Alexis, MHSc, PhD^{3,4} - <https://orcid.org/0000-0002-9417-8269>, David B. Peden, MD, MS^{3,4} - <https://orcid.org/0000-0003-4526-4627>, Jeffrey Roach, PhD⁵ <https://orcid.org/0000-0001-9817-5877>, Meghan E. Rebuli, PhD^{1,3,4} - <https://orcid.org/0000-0003-1918-2257>

¹Curriculum in Toxicology & Environmental Medicine, University of North Carolina at Chapel Hill, Chapel Hill, NC, United States

²Environmental Sciences and Engineering Department, Gillings School of Global Public Health, University of North Carolina at Chapel Hill, Chapel Hill, NC, United States

³Center for Environmental Medicine, Asthma and Lung Biology, University of North Carolina at Chapel Hill, Chapel Hill, NC, United States

⁴Department of Pediatrics, University of North Carolina at Chapel Hill, Chapel Hill, NC, United States

⁵UNC Microbiome Core, University of North Carolina at Chapel Hill, Chapel Hill, NC, United States

Corresponding author

Meghan E. Rebuli, PhD

4004A Mary Ellen Jones Building; CB 7325

116 Manning Drive

University of North Carolina at Chapel Hill

Chapel Hill, NC 27599

meradfor@email.unc.edu

Author Contributions: RD and MER conceived of and designed the study. MAA, NEA, DBP, and MER contributed to sample acquisition. CCU, RD, JD, and MER contributed to the analysis of the data. CCU, RD, NEA, DBP, JR, and MER contributed to data interpretation. CCU and MER created the initial manuscript draft. All authors reviewed the manuscript critically for important intellectual content and approved of the final version. All authors agree to be accountable for all aspects of the work in ensuring that questions related to the accuracy or integrity of any part of the work are appropriately investigated and resolved.

Funding: This work was supported by funding from the National Institute of Environmental Health Sciences (R21ES032928, K01ES032837, F31ES036437, R01ES025124, T32ES007126) and the Environmental Protection Agency (EPA-ORD-CPHEA-2021-01). The UNC Microbiome Core Facility is supported by the Center for Gastrointestinal Biology and Disease (CGIBD P30 DK034987) and the UNC Nutrition Obesity Research Center (NORC P30 DK056350). The use of RedCap was supported by the UNC North Carolina Translational and Clinical Sciences Institute through the National Center for Advancing Translational Sciences (NCATS) (UM1TR004406).

Running Head: Wood smoke alters sputum microbiome composition

Subject Category: 6.16 Pulmonary Toxicology

Total Word Count: 4700

At a Glance Commentary

Current Scientific Knowledge on the Subject: Wildfire-derived smoke has been associated with adverse respiratory conditions but, the mechanism by which this occurs is unknown. Previous studies using wood smoke as a model of wildfire smoke have focused on the respiratory immune response; however, the effect of wood smoke on the respiratory microbiome has not been examined.

What This Study Adds to the Field: This is the first controlled exposure study to examine the effect of wood smoke exposure on the human sputum microbiome using longitudinal sampling. We identified changes in sputum microbiome composition, which was also associated with changes in sputum macrophages.

Artificial Intelligence Disclaimer: No artificial intelligence tools were used in writing this manuscript.

This article has an online data supplement, which is accessible at the Supplements tab.

Abstract

Rationale: Wood smoke exposure is increasing worldwide due to the rise in wildfire events. Various studies have associated exposure to wildfire-derived smoke with adverse respiratory conditions. However, the mechanism by which this occurs is unknown. Previous studies using wood smoke as a model of wildfire smoke have focused on the respiratory immune response and have reported increased neutrophil percentage and cytokine production in airway samples. The effect of wood smoke on the respiratory microbiome, however, has not been examined.

Methods: Healthy volunteers (N=54) were subjected to controlled wood smoke exposure ($500 \mu\text{g}/\text{m}^3$) for two hours, and induced sputum samples were collected and processed for microbiome analysis, immune mediators, and cell differentials at baseline, six- and 24-hours post-exposure. A negative binomial mixed model analysis examined associations between microbiome components and inflammatory cells in sputum.

Main Results: Following wood smoke exposure, while sputum microbiome diversity remained unchanged, the microbiome composition was altered, particularly the abundance of several low-abundance bacteria, including *Fretibacterium* and *Selenomonas*, indicating that this inhalational exposure can alter the composition of the sputum microbiome. Additionally, a significant decrease in macrophage cells was observed at 24 hours without a significant change in neutrophils. We further found small but significant associations between different taxa and macrophages (per mg of sputum), including a negative association with *Fretibacterium*.

Conclusions: Together, these findings demonstrate that inhalational wood smoke exposure can modify several low-abundance bacteria within the respiratory microbiome and that these changes are associated with sputum inflammatory cell alterations, providing insights for future studies to focus on respiratory innate immune host-microbiome crosstalk in the context of environmental exposures.

Abstract Word Count: 249

Indexing terms (MeSH): Microbiota, Sputum, Wood, Smoke, Wildfires

Introduction

Wildfire events are increasing in magnitude and frequency in the United States (1,2) and many global regions (3–5). Wildfire-derived smoke has been reported to be more harmful to respiratory health than ambient particulate matter less than 2.5 micrometers in diameter ($PM_{2.5}$) from other sources (6,7), magnifying its global health threat status. Regarding respiratory health, the most common respiratory complications associated with exposure to wildfire smoke include asthma and chronic obstructive pulmonary disease exacerbations (8,9). Further, exposure to wildfire smoke has been linked to increased emergency department visits (10–13), hospital admissions (14,15), and mortality (16) due to respiratory complications. Given the increasing prevalence of wildfires and their associated health concerns, it is essential to understand the mechanisms by which wildfire smoke deteriorates respiratory health.

Alterations in the respiratory immune response have emerged as a likely significant initiating mechanism for health effects. Controlled exposure studies involving healthy volunteers have reported increased airway neutrophil percentage 24 hours post-exposure, indicating an immediate respiratory immune response triggered by wood smoke exposure (17–19). Furthermore, *in vitro* studies with human bronchial epithelial cells exposed to wood smoke observed an increase in proinflammatory cytokines, mucins, and barrier dysfunction (20–22). Moreover, wood smoke exposure has been shown to decrease the viability and effective defense mechanisms of bronchoalveolar macrophages *in vitro*, *ex vivo*, and *in vivo* (23,24). These studies indicate a significant impact on the immune response and underscore that wood smoke significantly disrupts the respiratory environment, which could affect other components of the respiratory tract and potentially lead to adverse respiratory effects.

In addition to the effects on the respiratory immune components, prior *in vitro* and controlled exposure studies and epidemiologic studies also indicate wood smoke can alter the response to pathogens, particularly influenza virus, suggesting impaired host defense responses (25–28). Host defense is the respiratory tract's primary function against invading pathogens and toxicants. However, the impact of wood smoke on this defense response remains unclear. While wood smoke has been shown to impair innate immune cell

functions critical in the acute response to viral infections, it may also disrupt other protective components of the respiratory mucosa, such as the respiratory microbiome.

The respiratory microbiome, a major component of the respiratory tract (29), is closely related to human health (30). Changes in the respiratory microbiome, also known as respiratory dysbiosis, have been associated with airway inflammation and various diseases, including asthma, chronic obstructive pulmonary disease (COPD), and respiratory viral infections (31,32). In the context of inhalational exposures, cigarette smoke and PM_{2.5} have been shown to decrease airway microbiome diversity and alter its composition, which, in turn, has been associated with respiratory health issues like COPD (33) and upper airway inflammation (34). Similar changes, including decreased diversity, dysbiosis, and associations with the host immune response, have been noted in respiratory diseases (35–37), suggesting that the dysbiosis following inhalational exposures may be an intermediary step between acute respiratory responses and disease development. Furthermore, these studies suggest an active and dynamic communication between the microbiome and its host, potentially influencing each other's response to the exposure simultaneously and thus influencing respiratory health.

To our knowledge, the effect of wood smoke exposure on the respiratory microbiome and its host-microbiome interactions remains understudied. A better understanding of the effects of wood smoke on the respiratory microbiome could have significant implications for respiratory health and the eventual development of microbiome-based preventive and therapeutic strategies against this increasing public health concern. Understanding the intricate interplay between wood smoke exposure, the host immune response, and the respiratory microbiome is essential to protect the population from the respiratory health effects associated with this exposure.

In this study, we examined induced sputum samples from healthy individuals exposed to 500 µg/m³ of wood smoke for 2 hours. We evaluated the structure and composition of the sputum microbiome and changes in inflammatory cell populations and pro-inflammatory cytokine production in sputum. Additionally, we explored associations between microbiome components and the innate host defense response following

wood smoke exposure. Some of the results of these studies have been previously reported in the form of an abstract(s) (38–40).

Methods

Detailed methods can be found in the Supplementary Materials. The data utilized for this publication can be found in the NIH Sequence Read Archive (SRA) under accession number PRJNA1186211 (<https://www.ncbi.nlm.nih.gov/sra/PRJNA1186211>) (Reviewer access link: <https://dataview.ncbi.nlm.nih.gov/object/PRJNA1186211?reviewer=ktgniras29ukhn5u148fedfn0j>). The code for the analyses reported can be found in GitHub (https://github.com/UNC-CEMALB/woodsmoke_human_respiratory_microbiome.git) and the data sets at Dataverse (Reviewer access link: <https://dataverse.unc.edu/privateurl.xhtml?token=622aace2-1330-4ba0-8907-036095985aef>).

Study participants

The study population (N=54, Table 1) is a subset of participants from the SmokeScreen clinical study (NCT02767973) (17). This study was approved by the University of North Carolina Institutional Review Board (UNC IRB Numbers: 05-2528 and 15-1775).

Controlled exposure to wood smoke

Participants were exposed to 500 µg/m³ of wood smoke for two hours under controlled conditions, as described previously (19). To maximize exposure, participants alternated between 15 minutes of light exercise and 15 minutes of rest throughout the exposure period.

Induced sputum collection and processing

Induced sputum was collected and processed as previously (41). Baseline samples were collected at a screening visit, followed by collections at six- and 24 hours post-exposure (hpe).

Markers of respiratory inflammatory response to wood smoke exposure

Total cell counts and differentials were determined from the sputum cell fraction by hematocytometer with Trypan Blue staining and on Hema 3 stained cytopsin slides. The sputum cytokine profile was determined

from the DPBS-treated sputum supernatant using a multiplex ELISA (MesoScale Discovery, Rockville, MD).

DNA extraction and 16S ribosomal RNA (rRNA) gene amplification and sequencing

Total DNA was extracted from the DTT-treated sputum supernatants. Mock sputum samples (n=3) and extraction controls (n=7) were used as negative controls. DNA extraction was completed using the DNeasy PowerSoil Pro kit (Qiagen, Germany). Extracted DNA was sent to SeqCenter (SeqCenter LLC, PA, USA) for amplification and high-throughput sequencing. Samples were prepared using the Quick-16STM NGS Library Prep Kit (Zymo Research, USA) with phased primers targeting the V3-V4 region.

Bioinformatic analysis

Sequences were processed and taxonomy was assigned in QIIME2 with SILVA and extended Human Oral Microbiome Databases (eHOMD) (42)(43)(45). eHOMD data is featured in the results, and SILVA is reported in the supplemental material. Metadata, phylogenetic tree, and feature and taxa tables were imported into RStudio (version 0.99.6) (46) and all subsequent analyses and visualizations were carried out using R version 4.1.0 (48) in RStudio (49).

Data analysis

Host respiratory inflammatory response: Inflammatory cell and cytokine data were analyzed using a repeated measures one-way ANOVA with pairwise paired *t*-tests (aggregate analysis). For sex-stratified analysis, a repeated measures two-way ANOVA with pairwise *t*-tests was used. Normality was assessed using Q-Q plots (Supplementary Figure E1).

Microbiome diversity: Alpha diversity metrics were determined using the Shannon index and Faith's phylogenetic diversity index and evaluated using the same approach as above. Beta diversity was evaluated between exposure groups with and without metadata variables (e.g. sex) using a PERMANOVA.

Differential abundance analysis and host-microbiome associations: Differential abundance analysis was performed with a negative binomial mixed model (NBMM) controlling for age, sex, BMI, and asthma status

using a minimum prevalence of 20%. Other demographic factors were assessed as sensitivity analyses in the model but did not substantially alter the results (Supplementary Tables E6, 8, 10, and 12). To investigate potential host-microbiome associations between sputum macrophages and microbiome taxa, we applied the same NBMM model, including macrophage per sputum mg data as a covariate. Additionally, we performed a stratified analysis to examine host-microbiome associations further (55), comparing cytokine and inflammatory cell data by baseline median microbiome observed richness (low = ASV <126, high = ASV >126).

All *p*-values were corrected for multiple comparisons using the Benjamin-Hochberg false discovery rate (FDR) correction. Reported *p*-values are adjusted unless otherwise specified.

Results

Demographics of the study population

The study population consisted of 54 healthy non-smokers, including 36 female and 18 male participants, with a mean age of 27 years (Table 1). Most participants were white (74.1%), non-Hispanic (90.7%), and non-asthmatic (81.5%) females (66%).

Sputum inflammatory cell and cytokine response to acute wood smoke exposure

Following wood smoke exposure (24 hpe), we observed an increase (FDR-adjusted $p \leq 0.01$, repeated measures one-way ANOVA, $n = 45$) and a decrease (FDR-adjusted $p \leq 0.0001$, $n = 45$) in neutrophil and macrophage percentages, respectively (Figure 1A and 1C). However, when looking at the absolute number (cells per sputum mg), while there was no change in total cell counts across timepoints (Supplementary Figure E2), we observed that the increase in sputum neutrophil percentage may have been driven by a decrease (FDR-adjusted $p \leq 0.01$, repeated measures one-way ANOVA, $n = 45$) in sputum macrophage cells/mg and not by a concurrent robust increase in neutrophil cells/mg (Figure 1B and D). When stratified by sex (Supplementary Figure E3), the inflammatory cell response observed across time in the aggregate analysis (increase in neutrophil percentage and decrease in macrophage percentage) was driven by female

subjects (FDR-adjusted $p \leq 0.01$ and $p \leq 0.0001$, respectively, repeated measures two-way ANOVA, $n = 45$; 30 females and 15 males). In contrast, no significant change was observed in males.

Regarding the sputum cytokine profile (interleukin (IL)-8, IL-6, IL-1 β , and tumor necrosis factor alpha (TNF α)), no significant differences were observed across time following wood smoke exposure in the aggregate or stratified by sex analysis (Supplementary Figures E4 and 5). However, sex-based analysis (Supplementary Figure 5) shows that at 24 hours, females had significantly lower levels of sputum IL-8 (FDR-adjusted $p \leq 0.01$, repeated measures two-way ANOVA, $n = 35$; 20 females and 15 males) and IL-6 (FDR-adjusted $p \leq 0.05$, repeated measures two-way ANOVA, $n = 35$; 20 females and 15 males) in comparison to males.

Microbiome diversity

There were no significant changes across time for alpha diversity (Shannon diversity and Faith's phylogenetic diversity) following wood smoke exposure in the aggregate (Figure 2A-B) or by sex analysis (Supplementary Figure E6). Regarding beta diversity (Bray-Curtis dissimilarity; Figure 2C and Supplementary Figure E7), we observed that wood smoke exposure had a statistically significant effect on beta diversity (nominal $p \leq 0.001$, PERMANOVA, $n = 54$). However, this effect explained only a small proportion of the total variation in beta diversity (1.02%; Supplemental Table E3). This suggests that other factors not included in our model could influence beta diversity. Interestingly, the effect of wood smoke exposure did not vary significantly based on sex (Supplementary Table E4).

Sputum microbiome composition

Regarding the composition of the sputum microbiome (Figure 3), the most abundant phylum in all samples was *Firmicutes*, followed by *Proteobacteria* and *Bacteroidetes*. At the genus level, the most abundant bacteria were *Streptococcus*, followed by *Veillonella* and *Prevotella*. Additionally, with eHOMD, classification at the species level was possible. The most abundant species across all samples

were *Streptococcus* sp., *S. salivarius*, and *V. atypica*. Similar results were observed using the SILVA database as a taxonomic classifier (Supplementary Figure E8).

Differential abundance analysis following acute wood smoke exposure

Using the negative binomial mixed model (NBMM), we identified one genus, *Selenomonas*, that increased with exposure (FDR-adjusted $p = 0.0165$, $n = 170$ taxa) and one that decreased with exposure (FDR-adjusted $p = 0.0000676$, $n = 170$ taxa), *Fretibacterium* (Figure 4A and Supplementary Table E5). When analyzing the data at the species level, additional bacteria emerged (Figure 4B and Supplementary Table E7). Similar to the genus level analysis, two *Selenomonas* species (sp. HMT 478 and an unclassified species) increased with exposure, while an unclassified *Fretibacterium* decreased with exposure. Further, *Haemophilus influenzae* increased with exposure, while *Neisseria cinerea*, *Porphyromonas catoniae*, and unclassified *Parvimonas* decreased following wood smoke exposure (Figure 4B and Supplementary Table E7). Interestingly, most of these bacteria are low-abundance bacterial species (relative abundance <1%) yet belong to the most abundant phyla identified in the respiratory tract (*Firmicutes*, *Proteobacteria*, and *Bacteroidetes*), except for *Fretibacterium*, which belongs to the *Synergistetes* phyla. The results obtained with SILVA also show an increase in *Selenomonas* and a decrease in *Fretibacterium* (Supplementary Figure E9 and Supplementary Tables E13 and 14).

Host-microbiome associations following acute wood smoke exposure

We assessed the potential relationship between the changes in differential abundance and altered respiratory inflammatory biomarkers to identify potential points of microbe-host crosstalk. To do this, we added macrophage per sputum mg data to the NBMM. We observed numerous small but significant associations between microbiome components and respiratory inflammatory cells (Figure 5 and Supplementary Tables E9-11). For instance, *Fretibacterium* was negatively associated with macrophages/mg (FDR-adjusted $p=0.00534$, $n = 450$ taxa). To further investigate host-microbiome associations, we compared cytokine and inflammatory cell responses to wood smoke exposure between high and low observed richness groups (Figure 6). These groupings revealed a similar response to the aggregate analysis (Figure 1 and Supplementary Figure E4). Notably, macrophages per sputum mg (Figure 5D) were significantly decreased only in the high observed richness group (FDR-adjusted $p \leq 0.05$, repeated measures one-way ANOVA, $n = 27$). No significant differences across time were observed regarding cytokine data (Supplementary Figure E10), similar to our aggregate analysis.

Discussion

In this controlled wood smoke exposure study of healthy adult participants, our results demonstrate significant alterations in respiratory microbiome composition and sputum inflammatory cells with wood smoke exposure. We identified that increases in the proportion of neutrophils are driven by significant decreases in the absolute number of sputum macrophages, without concurrent significant increases in the absolute number of neutrophils. We novelly report changes in sputum microbiome with exposure to acute wood smoke, particularly in low abundance genera and species. Changes in genera were robust to database choice (SILVA and eHOMD) and did not change with consideration of demographic factors, such as sex. We also identified associations between components of the sputum microbiome and the immune cell response to wood smoke. These findings provide evidence of the potential for wood smoke exposure to alter the respiratory microbiome composition and affect lung health.

Regarding the host inflammatory cell response, acute wood smoke exposure induced significant changes in two key inflammatory cells: neutrophils and macrophages. The increase in sputum neutrophil percentage has been documented previously (17,19,56). However, to our knowledge, no prior studies have reported that this increase in neutrophil percentage was driven by a significant decrease in the absolute number of macrophages (per sputum mg) and not an increase in absolute neutrophils (per sputum mg). This importantly highlights macrophages as an impacted, but understudied, player in the host response to wood smoke (Figure 1) and emphasizes the need for transparent reporting of total cell counts, in addition to transformed data for comparison across studies (57). It is possible that prior controlled wood smoke studies (17) only identified changes in percent neutrophils rather than a change in cells per mg due to reduced power and interindividual variability with a smaller N than used here. A previous study by Swiston et al. (2008) reported a slight, non-significant decrease in sputum macrophage percentage in firefighters 4 hours following wood smoke exposure (56). Similarly, in our study, the observed decrease in macrophage percentage and cells/mg was not evident at 6 hours post-exposure but became apparent at 24 hours. Previous studies have also reported impaired macrophage function and high toxicity following wood smoke exposure (23,58,59), potentially suggesting increased macrophage cell death and an explanation for the reduction in macrophage numbers we observe here. Together, these observations point towards macrophages as components of the respiratory response to acute wood smoke exposure that require further study. Interestingly, when stratified by sex, this same outcome (decreased macrophages) was observed in female but not male participants (Supplementary Figure E3), suggesting a sex-based differential response or susceptibility. Sex-based differences regarding wood smoke exposure have been previously reported (28).

Despite cellular changes, we observed no significant alterations in the cytokine profile following wood smoke exposure in our aggregate analysis (Supplementary Figure E4). Although these findings are consistent with similar exposure studies by Ghio et al. (2012) and Alexis et al. (2022), the reason behind the lack of alterations in the cytokine profile with observed immune cell changes remains unclear. Extending the observation time points beyond 24 hours might provide additional clarity, as a previous study

in guinea pigs reported an increase in various proinflammatory cytokines in the bronchoalveolar lavage 72 hours post-exposure (60). It is also possible that cytokines other than those we evaluated were altered, such as IL-33 (61) (62). In our study, when stratified by sex, we observed significantly lower levels of IL-8 and IL-6 in females compared to males at the 24-hour time point. Although not significant, we also observed an increasing trend in IL-6 and IL-8 across time in males but not females (Supplementary Figure E5), which may reach significance with an additional longitudinal timepoint. Our findings further suggest a difference in the response to wood smoke between males and females, warranting further in-depth studies.

In addition to the host response, this study aimed to evaluate the effect of wood smoke on the sputum microbiome. Our results suggest that the microbiome structure is resistant to acute wood smoke exposure, as evidenced by the lack of significant differences in alpha diversity (Figure 2A-B) and the small proportion of the total variation in beta diversity explained by the time post-exposure (1.02%; Supplemental Table E3) in our aggregate analysis. These results were also consistent in sex-stratified analyses (Supplementary Figure E6 and Supplementary Table E4). To our knowledge, only one previous human study has examined the effect of biomass smoke on the respiratory microbiome, albeit the focus was chronic exposure (63). This study reported no alpha and beta diversity differences, similar to our findings. In animal studies, chronic exposure to wood smoke resulted in decreased alpha diversity in the gut (64). However, another animal study on carbon black and ozone, common wood smoke components, reported disparate gut and lung microbiome responses, with gut microbiome changes not necessarily mirroring those in the respiratory tract (65), which underscores the importance of evaluating the respiratory microbiome response to inhalational exposures. The same study found that while one-day exposures to carbon black or ozone did not affect alpha diversity, four-day exposures did decrease it (Shannon index). These studies support that the microbiome structure may resist acute wood smoke exposure up to a threshold. This indicates some microbiome resiliency or flexibility and its potential beneficial or protective role in lung health.

Regarding microbiome composition at baseline (Figure 3), we observed profiles similar to those reported by other respiratory microbiome studies. In our analysis, the most abundant phylum was *Firmicutes*, a

common finding in the respiratory tract of healthy adults (29). Similarly, at the genus level, *Streptococcus*, *Prevotella*, and *Veillonella* were the most abundant taxa, also commonly found in the oropharynx (29). Using eHOMD (45), we reached species resolution, the top five most abundant species being *Streptococcus* sp., *S. salivarius*, *Veillonella atypica*, *Neisseria* sp., and *Haemophilus parainfluenzae*. Notably, because of how induced sputum is expelled from the oral cavity, its sampling location in the central airway, and the potential contribution of micro-aspiration from the oral cavity to the microbiome of the central airway (66), sputum is likely a mixture of cells, microbes, and secretions from both the upper and central airway (67,68). However, the taxa identified in this study have been reported as common components of the respiratory microbiome, such as in studies examining bronchoalveolar lavage (BAL) samples, which are less prone to oral contaminants as a sampling method, thus providing confidence in our observed results and their biological relevance (69,70). Future research is needed to parse out the effects of wood smoke exposure on other components of the airway, such as BAL and the oral cavity to determine whether effects across the airway differ based on compartment.

Importantly, as mentioned in our methods section, we used two taxonomic classifiers: eHOMD and SILVA. We observed similar results in our microbiome composition analysis at the phylum and genus levels using both classifiers. However, at the species level, SILVA could not identify most bacteria and classified them as unidentified, whereas eHOMD identified a higher number of bacterial species. This is most likely due to the specificity of the eHOMD database to our analyzed sample, which focuses on bacteria in the aerodigestive tract (45).

While we did not identify changes in microbiome diversity, our results indicate the differential abundance of specific taxa post-exposure. This is similar to a prior study, where changes in the relative abundance of specific bacteria without changes in diversity were observed (63). Together, these and our findings indicate that certain taxa are becoming more or less abundant (dysbiotic) within the consistent overall structure of the respiratory microbiome following smoke exposure. Notably, our differential abundance analysis shows that wood smoke mostly affected low-abundance bacteria, those in the <1% abundance group (Figure 3).

At the genus level, we observed a decrease in *Fretibacterium* and an increase in *Selenomonas* (Figure 4A and Supplementary Table E5 and 6). To our knowledge, this is the first report on the decreased abundance of *Fretibacterium* in the context of environmental exposures. Although there is not much information on this currently uncultivable bacterium, its increased abundance has been associated with periodontitis and gingival bleeding (71–73). *Selenomonas* is an opportunistic pathogen, and its increased abundance, along with that from other taxa, has been observed in the oral microbiota of subjects with COPD derived from tobacco smoke and biomass smoke exposure (74). At the species level (Figure 4B and Supplementary Table E7 and 8), *H. influenzae* and two species of *Selenomonas* increased post-exposure. On the other hand, *Neisseria cinerea*, *Porphyromonas catoniae*, and unclassified *Fretibacterium* and *Parvimonas* decreased following exposure. Most of these bacteria, except for *Selenomonas*, were low-abundance bacteria. Low-abundance taxa have been reported to be essential for maintaining a stable respiratory microbiome network (75) and immunostimulatory compared to abundant bacteria, making them important immune response modulators (76). These studies suggest that the changes observed in low-abundance bacteria can affect the overall microbiome composition and the host immune response, potentially leading to adverse outcomes. However, establishing a causal link between altered low abundance taxa and the development of respiratory disease with exposure to wildfire smoke requires more research in the future.

As mentioned, a notable observation was the significant changes observed in low-abundant bacteria, many of which are typically isolated or described in the oral cavity and linked to oral disease. As previously discussed, while some degree of oral contamination in induced sputum samples is inevitable, oral diseases and associated taxa have been linked to respiratory disease. Previous studies have associated oral disease with respiratory disease, such as periodontitis with COPD (77,78) and asthma (79). The latter study further identified high levels of *Prevotella intermedia* with severe asthma. These findings emphasize the connection between oral and respiratory health, suggesting that bacteria in the oral and airway microbiomes could significantly influence respiratory health. Consequently, the oral microbiome could be used as a

biomarker for susceptibility to inhalational exposures and respiratory disease; however, much more research would be needed to confirm this hypothesis.

Due to the hypothesized link between the microbiome and host immune response to pollutants, we also looked for associations between components of the sputum microbiome and cellular immune mediators of the respiratory tract, specifically, macrophages per sputum mg (Figure 5 and Supplementary Tables E9-12). We identified small but significant associations between various taxa and sputum macrophages. These taxa included the differentially abundant bacteria previously identified, *Fretibacterium* and *Selenomonas* HMT 478, which were negatively associated with sputum macrophages. The biological relevance of these findings needs to be further explored in future studies, including *in vitro* approaches. The gap between microbial taxa and cells may be too large to draw direct conclusions. Investigating metabolites as intermediaries may help bridge this gap and provide a clearer understanding of underlying mechanisms.

To further investigate host-microbiome associations, we compared the cytokine and inflammatory cell data between high and low baseline observed richness groups (Figure 6 and Supplementary Figure E10). This approach was informed by a previous study that reported a relationship between lower airway microbiome richness and the cytokine response to diesel exhaust exposure (55). In our study, we observed a decrease in macrophages per sputum mg only in the high-richness group (Figure 6D), suggesting that baseline microbiome structure may influence the host response to wood smoke. This finding supports the potential for microbiome richness to serve as a biomarker of susceptibility in future studies. While it remains unclear whether the decrease in macrophages is beneficial or detrimental to the host, or at what point it might become harmful, this observation provides valuable insights into the need for further investigation of microbiome and macrophage interaction in the airways.

Limitations: Our study has several important limitations to consider when applying and translating results. First, this study focuses on healthy volunteers undergoing light exercise. The sputum microbiome of susceptible populations or individuals not undergoing exercise could respond differently to exposure. Second, we utilized induced sputum for cell differentials. As the dilution of samples from induced sputum

is difficult to control for, differences in sampling by subject may influence data variability. Third, we used DTT-treated sputum supernatants for our microbiome analysis rather than raw sputum samples based on sample availability and included limited numbers of negative controls to account for procedural background sequences. Additional controls would have aided further in detecting potential contaminants. However, based on the similarity of our relative abundance analyses to prior studies, we are confident that the differences detected here are of biological relevance. Additionally, oral contamination is an inherent limitation of induced sputum due to the collection method, which involves passing through the oral cavity. As a result, the likelihood of oral microbiota contributing to the observed taxa is high, as several of our identified taxa are often associated with the oral cavity. However, some of the taxa we identified have also been reported in studies with BAL and bronchial brushings, which are less likely to be contaminated by the oral cavity, suggesting that it is possible that the taxa more commonly identified in oral microbiome studies in our results are indeed present and modified in the airway with wood smoke exposure (69,70,80). Future studies should confirm these findings by collecting paired oral, sputum, and BAL samples to address this limitation. Our study also uses a modest sample size ($n = 54$). Thus, our study resolution may not be sufficient to detect all biologically relevant differences with exposure. Related to the latter, our ability to detect statistically significant male effects may have been limited by the smaller sample size in this subgroup, highlighting the need for future studies with larger, sex-balanced cohorts. Additionally, our exposure consisted of smoldered red oak, which may limit the application of findings to other fuel types and mixtures. Finally, regarding host-microbiome associations, changes in microbiome structure and composition do not necessarily reflect changes in functionality. Therefore, future studies including markers of function, such as metabolome, are needed.

Conclusion

These results represent a significant advancement in understanding the impact of wood smoke exposure on respiratory health by focusing on the respiratory microbiome as a crucial component for airway homeostasis. Our findings novelly highlight that several low-abundance bacterial species and no highly

abundant species were affected by acute controlled wood smoke exposure, which, based on previous studies, could have significant health implications. Additionally, we highlight macrophages as key players in the host response to this exposure. Notably, we identified significant associations between several taxa and sputum macrophages, providing valuable insight for future research to explore the mechanism behind these associations and host-microbiome interactions. To our knowledge, this is the first study in humans to evaluate and identify the effects of acute wood smoke exposure on the sputum microbiome, highlighting a novel endpoint that may contribute to environmental exposure-related lung health.

Tables and Figures

Table 1. Study population demographics.

Characteristic	Overall, N = 54¹	Sex	
		Female, N = 36¹	Male, N = 18¹
Age	27.4 (6.5)	26.3 (6.4)	29.4 (6.5)
BMI	25.2 (5.3)	25.1 (5.6)	25.6 (4.6)
Race			
White	40 (74%)	28 (78%)	12 (67%)
Black	7 (13%)	5 (14%)	2 (11%)
Asian	4 (7.4%)	2 (5.6%)	2 (11%)
Other	3 (5.6%)	1 (2.8%)	2 (11%)
Ethnicity			
Non-Hispanic/Latino	49 (91%)	33 (92%)	16 (89%)
Hispanic/Latino	5 (9.3%)	3 (8.3%)	2 (11%)
Asthmatic	10 (19%)	7 (19%)	3 (17%)

¹Mean (SD); n (%)

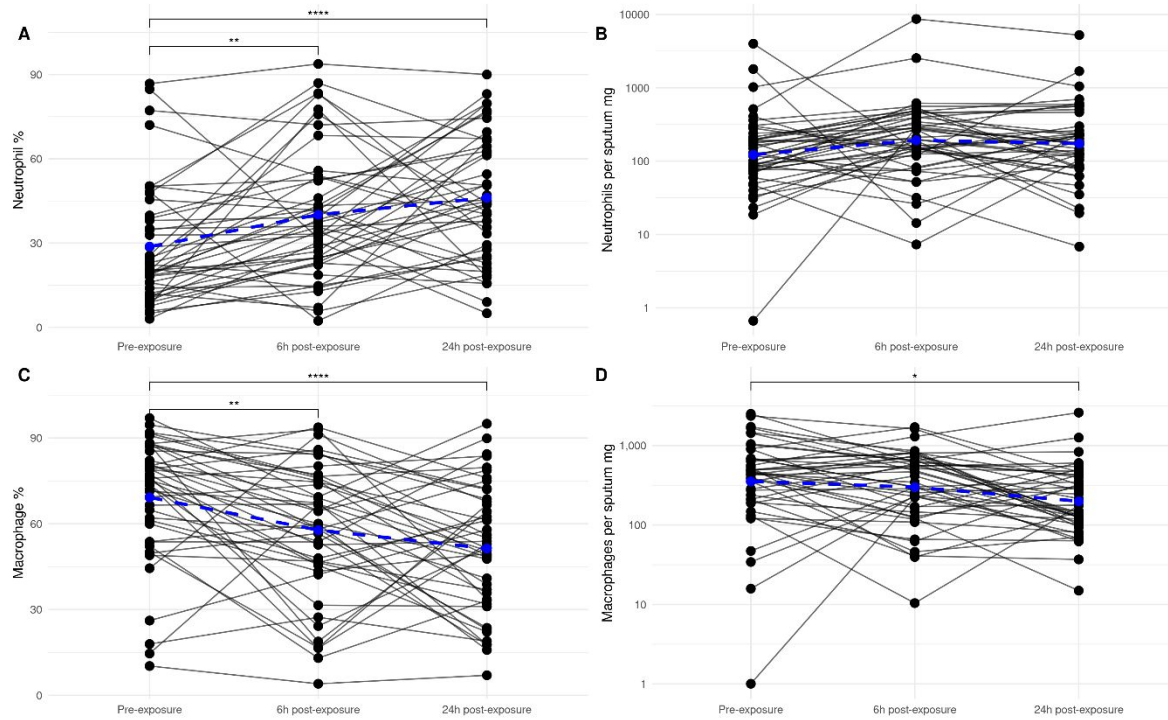


Figure 1. Sputum inflammatory cell host response following wood smoke exposure. Induced sputum cell differentials were stained and counted for neutrophils and macrophages prior to exposure (Pre-exposure), at six hours post-exposure (6h post-exposure), and at 24 hours post-exposure (24h post-exposure). A) Relative percentage of neutrophils, B) absolute neutrophils per mg of sputum, C) relative percentage of macrophages, and D) absolute macrophages per mg of sputum are shown as individual data points connected by lines to represent paired analysis for each subject. The blue dashed line represents the mean. Analyzed with repeated measures one-way ANOVA followed by pairwise paired t-tests. P-values shown ($(*)P \leq 0.05$, $(**)P \leq 0.01$, and $(****)P \leq 0.0001$) correspond to the paired t-test results.

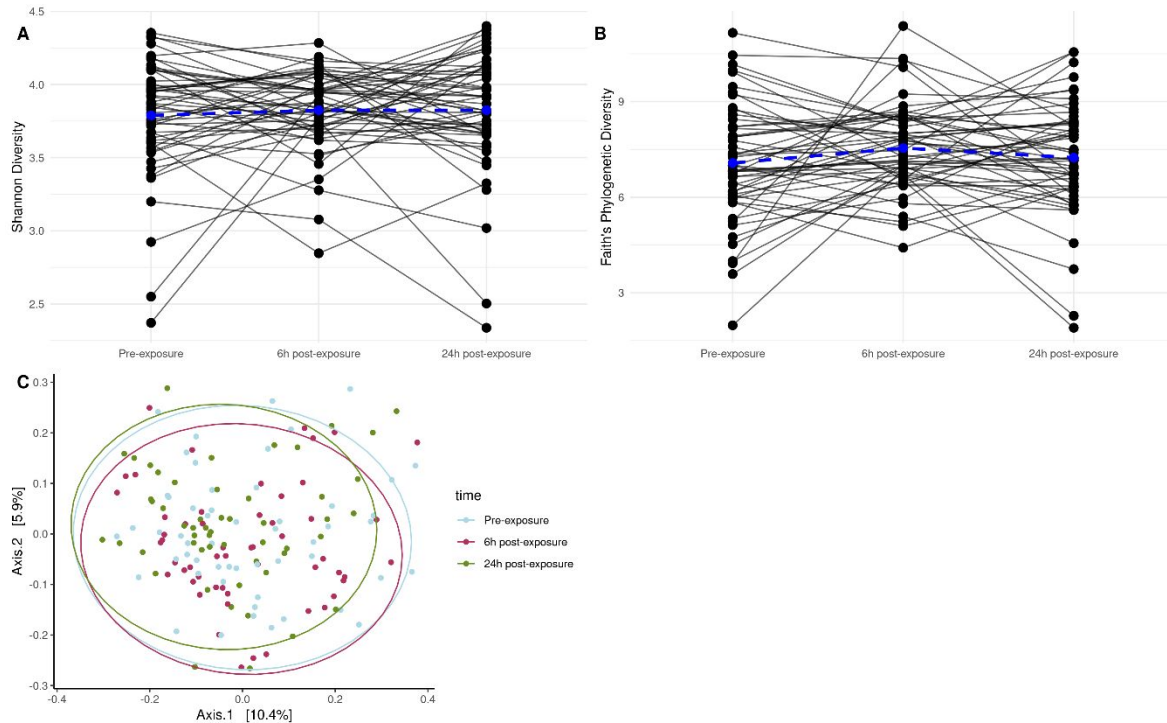


Figure 2. Sputum microbiome diversity with exposure to wood smoke. Induced sputum supernatants were analyzed via 16S rRNA sequencing. Samples prior to exposure (Pre-exposure), at six hours post-exposure (6h post-exposure), and at 24 hours post-exposure (24h post-exposure) were evaluated for differences in alpha and beta diversity. Alpha diversity was analyzed by Shannon's (A) and Faith's (B) indices. Alpha diversity data are presented as individual data points connected by lines to represent paired analysis for each subject. The blue dashed line represents the mean. Beta diversity was assessed using Bray-Curtis (C) and presented as a PCoA. No significant differences were detected in alpha diversity. A statistically significant but small effect was observed in beta diversity ($P \leq 0.001$), accounting for 1.02% of the total variation by exposure.

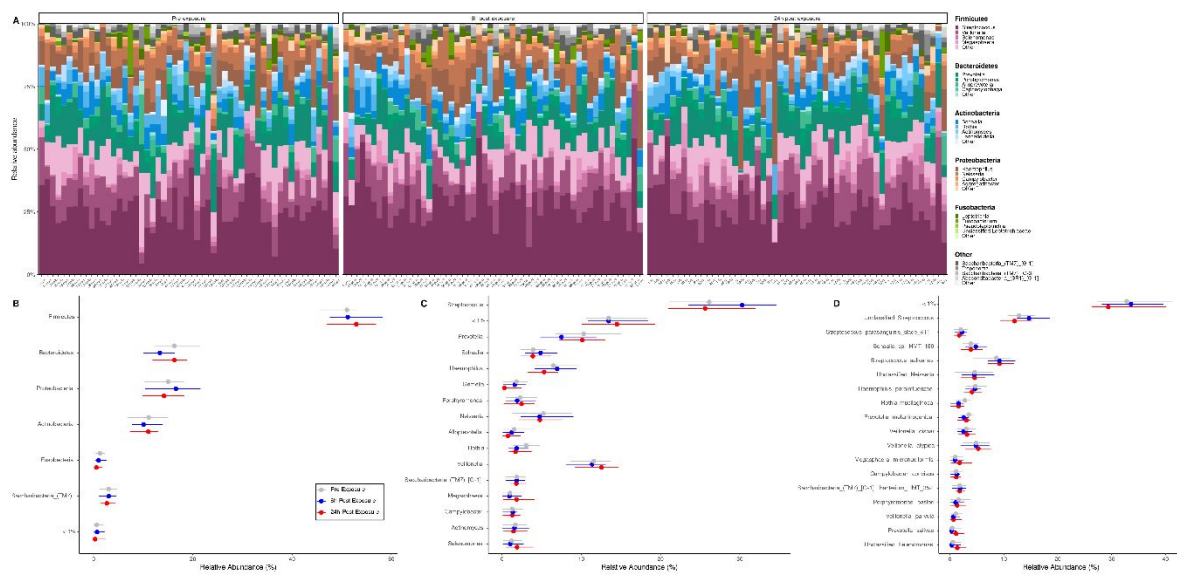


Figure 3. Sputum microbiome composition. Induced sputum supernatants from study participants exposed to wood smoke were collected Pre-exposure, 6h post-exposure, and 24h post-exposure. Samples were analyzed via 16S rRNA sequencing and annotated using eHOMD. (A) Microbiome composition by relative abundance is shown at the genus level with each bar representing an individual participant's composition. (B-D) Aggregate median relative abundances at the (B) phylum, (C) genus, and (D) species level. Dots represent the median and error bars represent the interquartile range. Relative abundance is shown for pre-exposure (gray), 6h post-exposure (blue) and 24h post-exposure (red). The <1% group on the y-axis of B, C, and D represent combined taxa that account for less than 1% relative abundance.

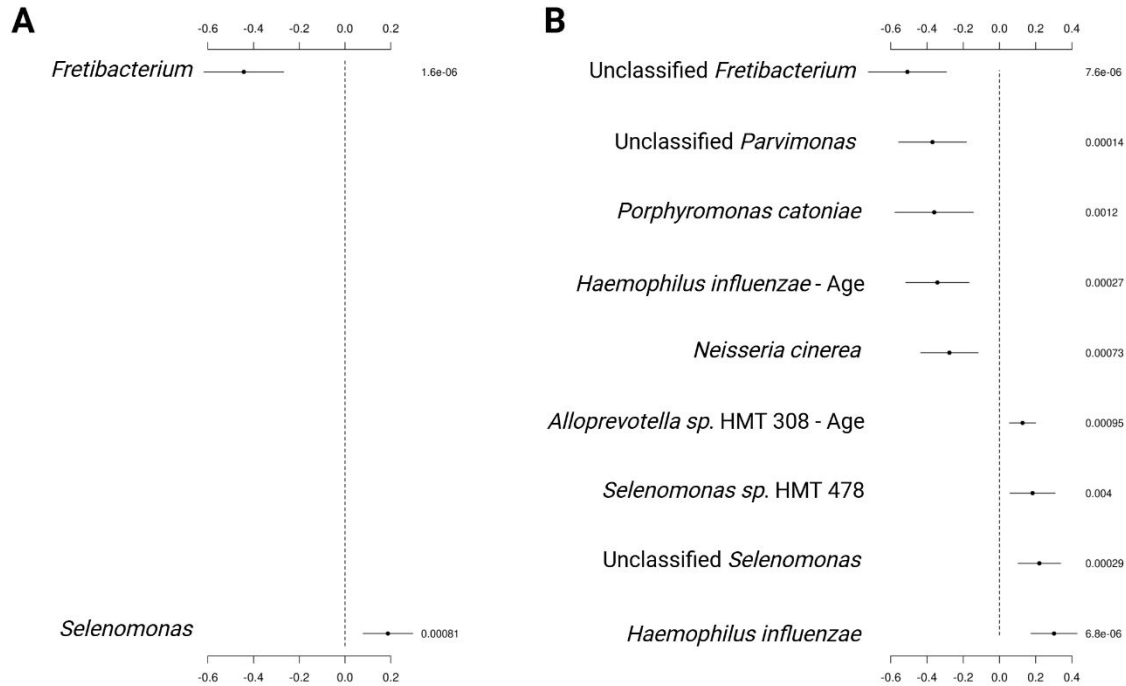


Figure 4. Sputum microbiome differential abundance analysis for the effects of wood smoke exposure at the (A) genus and (B) species level using eHOMD and a negative binomial mixed model (NBMM) controlling for age, sex, BMI (body mass index), and asthma status. The analysis was performed using microbiome count data. Bacteria significantly affected by exposure are listed on the left of each plot. the magnitude and direction of the effect are shown in the middle of each plot, with associated p-values on the right. Positive coefficient values (to the right of the dashed line) indicate enrichment following exposure, while negative coefficients indicate a decrease in abundance. Only taxa with significant adjusted p-values (FDR < 0.05, Benjamini-Hochberg correction) are displayed. The p-values shown in the figure represent the unadjusted values. The coefficient estimates are plotted along the x-axis, and the error bars represent 95% confidence intervals around these estimates.

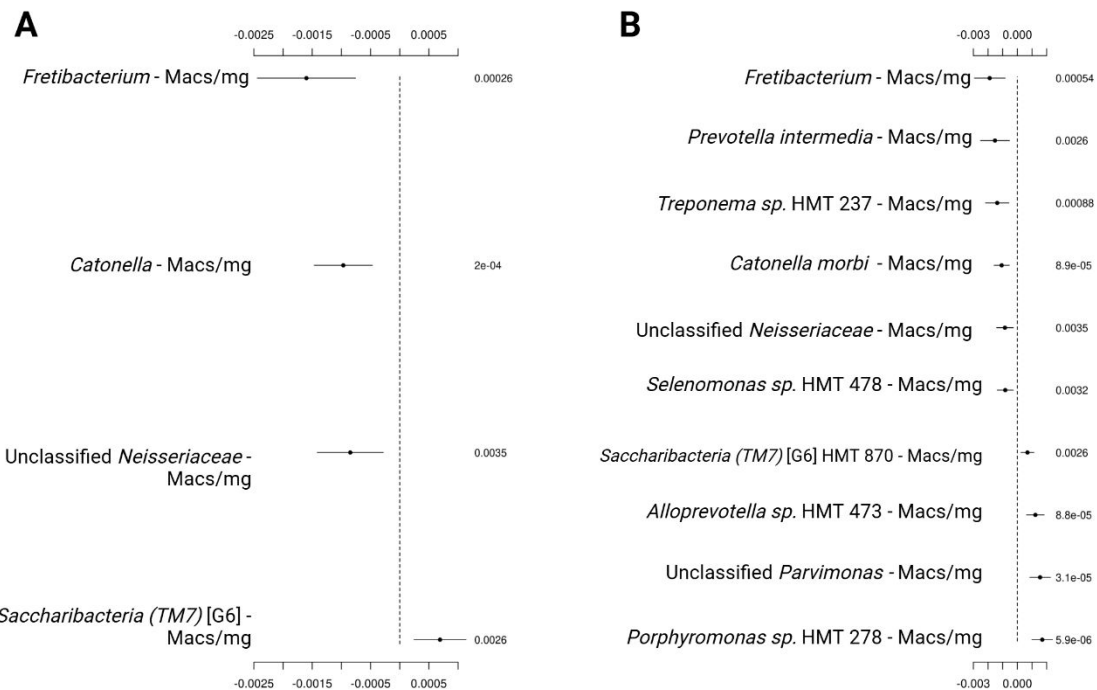


Figure 5. Sputum host-microbiome associations following wood smoke exposure at the genus (A) and species (B) level using eHOMD and a negative binomial mixed model (NBMM), which included inflammatory cells as an interactive factor, controlling for age, sex, BMI (body mass index), and asthma status. The analysis was performed using microbiome count data and inflammatory cell absolute counts. Bacteria and inflammatory cell associations significantly affected by exposure are listed on the left of each plot (microbe-cell type; Macs = Macrophages/sputum mg). The direction and magnitude of the effect are shown in the middle of each plot, with associated p-values on the right. Positive coefficients (to the right of the dashed line) indicate enrichment following exposure, while negative coefficients indicate a decrease in abundance. Only taxa with significant adjusted p-values (FDR < 0.05, Benjamini-Hochberg correction) are displayed. The p-values shown in the figure represent the unadjusted values. The coefficient estimates are plotted along the x-axis, and the error bars represent 95% confidence intervals around these estimates.

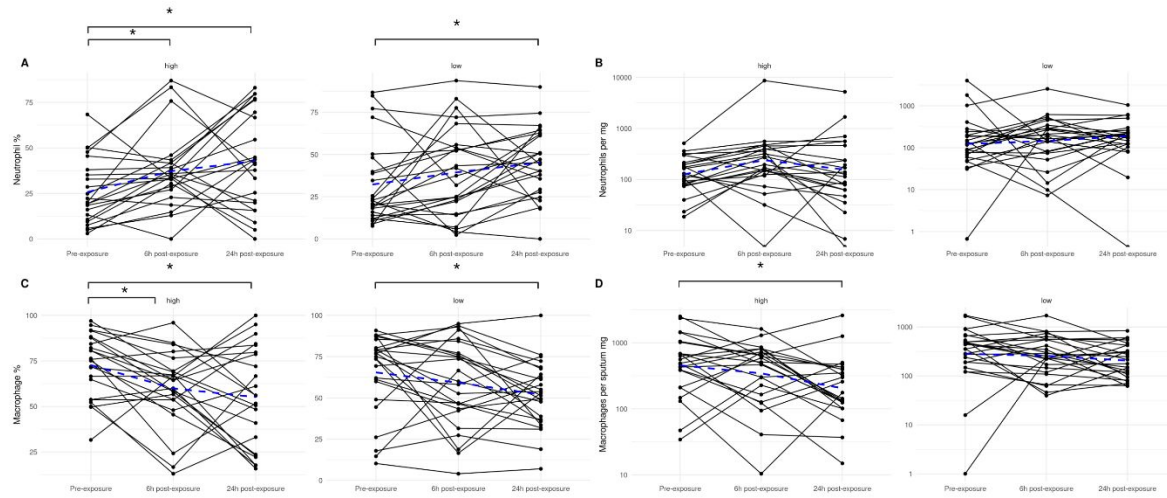


Figure 6. Host inflammatory cell response to wood smoke exposure stratified by baseline microbiome richness. Induced sputum cell differentials were stained and counted for neutrophils and macrophages prior to exposure (Pre-exposure), at six hours post-exposure (6h post-exposure), and at 24 hours post-exposure (24h post-exposure). A) Relative percentage of neutrophils, B) absolute neutrophils per mg of sputum, C) relative percentage of macrophages, and D) absolute macrophages per mg of sputum are shown as individual data points connected by lines to represent paired analysis for each subject. The blue dashed line represents the mean. Analyzed with repeated measures one-way ANOVA followed by pairwise paired t-tests. P-values shown ((*P≤0.05) correspond to the paired t-test results.

References

1. Iglesias V, Balch JK, Travis WR. U.S. fires became larger, more frequent, and more widespread in the 2000s. *Sci Adv.* 2022;8(11):eabc0020.
2. US EPA O. Climate Change Indicators: Wildfires [Internet]. 2016 [cited 2024 May 20]. Available from: <https://www.epa.gov/climate-indicators/climate-change-indicators-wildfires>
3. El Garroussi S, Di Giuseppe F, Barnard C, Wetterhall F. Europe faces up to tenfold increase in extreme fires in a warming climate. *Npj Clim Atmospheric Sci.* 2024 Jan 29;7(1):1–11.
4. Senande-Rivera M, Insua-Costa D, Miguez-Macho G. Spatial and temporal expansion of global wildland fire activity in response to climate change. *Nat Commun.* 2022 Mar 8;13(1):1208.
5. Wimberly MC, Wanyama D, Doughty R, Peiro H, Crowell S. Increasing Fire Activity in African Tropical Forests Is Associated With Deforestation and Climate Change. *Geophys Res Lett.* 2024;51(9):e2023GL106240.
6. Aguilera R, Corringham T, Gershunov A, Benmarhnia T. Wildfire smoke impacts respiratory health more than fine particles from other sources: observational evidence from Southern California. *Nat Commun.* 2021 Mar 5;12(1):1493.
7. Wegesser TC, Pinkerton KE, Last JA. California wildfires of 2008: coarse and fine particulate matter toxicity. *Environ Health Perspect.* 2009 Jun;117(6):893–7.
8. Alman BL, Pfister G, Hao H, Stowell J, Hu X, Liu Y, et al. The association of wildfire smoke with respiratory and cardiovascular emergency department visits in Colorado in 2012: a case crossover study. *Environ Health.* 2016 Jun 4;15(1):64.
9. Horne BD, Johnson MM, Blagev DP, Haddad F, Knowlton KU, Bride D, et al. Association of Short-term Increases in Ambient Fine Particulate Matter With Hospitalization for Asthma or COPD During Wildfire Season and Other Time Periods. *CHEST Pulm.* 2024 Mar 29;100053.
10. Chen AI, Ebisu K, Benmarhnia T, Basu R. Emergency department visits associated with wildfire smoke events in California, 2016–2019. *Environ Res.* 2023 Dec 1;238(Pt 1):117154.
11. Heft-Neal S, Gould CF, Childs ML, Kiang MV, Nadeau KC, Duggan M, et al. Emergency department visits respond nonlinearly to wildfire smoke. *Proc Natl Acad Sci U S A.* 2023 Sep 26;120(39):e2302409120.
12. Thilakaratne R, Hoshiko S, Rosenberg A, Hayashi T, Buckman JR, Rappold AG. Wildfires and the Changing Landscape of Air Pollution-related Health Burden in California. *Am J Respir Crit Care Med.* 2023 Apr 1;207(7):887–98.
13. Belz DC, Myers LC, Hansel NN. Cardiopulmonary Health Burden of Wildfire Particulate Exposure Urges Us to Consider Interventions. *Am J Respir Crit Care Med.* 2023 Apr 1;207(7):807–9.
14. Liu JC, Wilson A, Mickley LJ, Dominici F, Ebisu K, Wang Y, et al. Wildfire-specific Fine Particulate Matter and Risk of Hospital Admissions in Urban and Rural Counties. *Epidemiol Camb Mass.* 2017 Jan;28(1):77–85.

15. Ye T, Guo Y, Chen G, Yue X, Xu R, Coêlho M de Szs, et al. Risk and burden of hospital admissions associated with wildfire-related PM_{2.5} in Brazil, 2000–15: a nationwide time-series study. *Lancet Planet Health.* 2021 Sep 1;5(9):e599–607.
16. Ye T, Xu R, Yue X, Chen G, Yu P, Coêlho MSzs, et al. Short-term exposure to wildfire-related PM_{2.5} increases mortality risks and burdens in Brazil. *Nat Commun.* 2022 Dec 10;13(1):7651.
17. Alexis NE, Zhou LY, Burbank AJ, Almond M, Hernandez ML, Mills KH, et al. Development of a screening protocol to identify persons who are responsive to wood smoke particle-induced airway inflammation with pilot assessment of GSTM1 genotype and asthma status as response modifiers. *Inhal Toxicol.* 2022;34(11–12):329–39.
18. Burbank AJ, Hernandez ML, Mills KH, Alexis N, Alt EM, Zhou H, et al. Characterizing Airway Inflammatory Responses to Wood-Smoke Inhalation. *J Allergy Clin Immunol.* 2019 Feb 1;143(2):AB23.
19. Ghio AJ, Soukup JM, Case M, Dailey LA, Richards J, Berntsen J, et al. Exposure to wood smoke particles produces inflammation in healthy volunteers. *Occup Environ Med.* 2012 Mar 1;69(3):170–5.
20. Memon TA, Nguyen ND, Burrell KL, Scott AF, Almestica-Roberts M, Rapp E, et al. Wood Smoke Particles Stimulate MUC5AC Overproduction by Human Bronchial Epithelial Cells Through TRPA1 and EGFR Signaling. *Toxicol Sci.* 2020 Apr;174(2):278–90.
21. Roscioli E, Hamon R, Lester SE, Jersmann HPA, Reynolds PN, Hodge S. Airway epithelial cells exposed to wildfire smoke extract exhibit dysregulated autophagy and barrier dysfunction consistent with COPD. *Respir Res.* 2018 Nov 28;19(1):234.
22. Wang B, Chen H, Xenaki D, Liao J, Cowie C, Oliver BG. Differential inflammatory and toxic effects in-vitro of wood smoke and traffic-related particulate matter from Sydney, Australia. *Chemosphere.* 2021 Jun 1;272:129616.
23. Hansson A, Rankin G, Uski O, Friberg M, Pourazar J, Lindgren R, et al. Reduced bronchoalveolar macrophage phagocytosis and cytotoxic effects after controlled short-term exposure to wood smoke in healthy humans. Part Fibre Toxicol. 2023 Jul 31;20(1):30.
24. Migliaccio CT, Kobos E, King QO, Porter V, Jessop F, Ward T. Adverse effects of wood smoke PM_{2.5} exposure on macrophage functions. *Inhal Toxicol.* 2013 Feb;25(2):67–76.
25. Brocke SA, Billings GT, Taft-Benz S, Alexis NE, Heise MT, Jaspers I. Woodsmoke particle exposure prior to SARS-CoV-2 infection alters antiviral response gene expression in human nasal epithelial cells in a sex-dependent manner. *Am J Physiol-Lung Cell Mol Physiol.* 2022 Mar;322(3):L479–94.
26. Gordon SB, Bruce NG, Grigg J, Hibberd PL, Kurmi OP, Lam K bong H, et al. Respiratory risks from household air pollution in low and middle income countries. *Lancet Respir Med.* 2014 Oct;2(10):823–60.
27. Landguth EL, Holden ZA, Graham J, Stark B, Mokhtari EB, Kaleczyc E, et al. The delayed effect of wildfire season particulate matter on subsequent influenza season in a mountain west region of the USA. *Environ Int.* 2020 Jun 1;139:105668.

28. Reboli ME, Speen AM, Martin EM, Addo KA, Pawlak EA, Glista-Baker E, et al. Wood Smoke Exposure Alters Human Inflammatory Responses to Viral Infection in a Sex-Specific Manner. A Randomized, Placebo-controlled Study. *Am J Respir Crit Care Med.* 2019 Abril;199(8):996–1007.
29. Man WH, de Steenhuijsen Piters WAA, Bogaert D. The microbiota of the respiratory tract: gatekeeper to respiratory health. *Nat Rev Microbiol.* 2017 May;15(5):259–70.
30. Manor O, Dai CL, Kornilov SA, Smith B, Price ND, Lovejoy JC, et al. Health and disease markers correlate with gut microbiome composition across thousands of people. *Nat Commun.* 2020 Oct 15;11(1):5206.
31. Li R, Li J, Zhou X. Lung microbiome: new insights into the pathogenesis of respiratory diseases. *Signal Transduct Target Ther.* 2024 Jan 17;9(1):1–27.
32. Xue Q, Xie Y, He Y, Yu Y, Fang G, Yu W, et al. Lung microbiome and cytokine profiles in different disease states of COPD: a cohort study. *Sci Rep.* 2023 Apr 7;13:5715.
33. Lin L, Yi X, Liu H, Meng R, Li S, Liu X, et al. The airway microbiome mediates the interaction between environmental exposure and respiratory health in humans. *Nat Med.* 2023 Jul;29(7):1750–9.
34. Li W, Sun B, Li H, An Z, Li J, Jiang J, et al. Association between short-term exposure to PM2.5 and nasal microbiota dysbiosis, inflammation and oxidative stress: A panel study of healthy young adults. *Ecotoxicol Environ Saf.* 2023 Sep 1;262:115156.
35. Chen M, He S, Miles P, Li C, Ge Y, Yu X, et al. Nasal Bacterial Microbiome Differs Between Healthy Controls and Those With Asthma and Allergic Rhinitis. *Front Cell Infect Microbiol.* 2022;12:841995.
36. Dicker AJ, Huang JTJ, Lonergan M, Keir HR, Fong CJ, Tan B, et al. The sputum microbiome, airway inflammation, and mortality in chronic obstructive pulmonary disease. *J Allergy Clin Immunol.* 2021 Jan 1;147(1):158–67.
37. Hufnagl K, Pali-Schöll I, Roth-Walter F, Jensen-Jarolim E. Dysbiosis of the gut and lung microbiome has a role in asthma. *Semin Immunopathol.* 2020;42(1):75–93.
38. Cobos-Uribe C, Dhingra R, Almond MA, Alexis NE, Peden DB, Roach J, et al. Wood smoke exposure and its effects on the respiratory microbiome. *Toxicol Suppl Toxicol Sci.* 2024;Abstract #PL2071:95.
39. Reboli M, Nalesnik M, Cobos-Uribe C, Payton A, Almond M, Robinette C, et al. Human airway Immune homeostasis and lung function are altered with controlled exposure to model wildfire smoke: characterizing susceptibility factors and the secretome. *Eur Respir J [Internet].* 2023 Oct 27 [cited 2024 Dec 10];62(suppl 67). Available from: https://publications.ersnet.org/content/erj/62/suppl_67/PA1600
40. Cobos-Uribe C. Controlled Wood Smoke Exposure Alters Human Central Airway Inflammatory Cell Profiles and Microbiome Composition: Evidence of Host-Microbiome Interaction. In Durham, NC.; 2024. Available from: <https://www.toxicology.org/groups/rc/nc/docs/2024-NCSOT-Annual-Meeting-Program.pdf>

41. Alexis N, Soukup J, Ghio A, Becker S. Sputum Phagocytes from Healthy Individuals Are Functional and Activated: A Flow Cytometric Comparison with Cells in Bronchoalveolar Lavage and Peripheral Blood. *Clin Immunol.* 2000 Oct 1;97(1):21–32.
42. Bolyen E, Rideout JR, Dillon MR, Bokulich NA, Abnet CC, Al-Ghalith GA, et al. Reproducible, interactive, scalable and extensible microbiome data science using QIIME 2. *Nat Biotechnol.* 2019 Aug;37(8):852–7.
43. Callahan BJ, McMurdie PJ, Rosen MJ, Han AW, Johnson AJA, Holmes SP. DADA2: High resolution sample inference from Illumina amplicon data. *Nat Methods.* 2016 Jul;13(7):581–3.
44. Quast C, Pruesse E, Yilmaz P, Gerken J, Schweer T, Yarza P, et al. The SILVA ribosomal RNA gene database project: improved data processing and web-based tools. *Nucleic Acids Res.* 2013 Jan 1;41(D1):D590–6.
45. Escapa IF, Chen T, Huang Y, Gajare P, Dewhirst FE, Lemon KP. New Insights into Human Nostril Microbiome from the Expanded Human Oral Microbiome Database (eHOMD): a Resource for the Microbiome of the Human Aerodigestive Tract. *mSystems.* 2018 Dec 4;3(6):e00187-18.
46. Bisanz JE. qiime2R: Importing QIIME2 artifacts and associated data into R sessions [Internet]. 2018 [cited 2024 Jun 18]. Available from: <https://github.com/jbisanz/qiime2R>
47. Davis NM, Proctor DM, Holmes SP, Relman DA, Callahan BJ. Simple statistical identification and removal of contaminant sequences in marker-gene and metagenomics data. *Microbiome.* 2018 Dec 17;6(1):226.
48. R Core Team. R: A Language and Environment for Statistical Computing [Internet]. Vienna, Austria: R Foundation for Statistical Computing; 2021. Available from: <https://www.R-project.org/>
49. Posit team. RStudio: Integrated Development Environment for R [Internet]. Boston, MA: Posit Software, PBC; 2023. Available from: <http://www.posit.co/>
50. McMurdie PJ, Holmes S. phyloseq: An R Package for Reproducible Interactive Analysis and Graphics of Microbiome Census Data. *PLOS ONE.* 2013 abr;8(4):e61217.
51. Battaglia, Thomas. GitHub. 2015 [cited 2024 Jun 18]. btools: A suite of R function for all types of microbial diversity analyses. Available from: <https://github.com/twbattaglia/btools/blob/master/README.md>
52. Oksanen J, Simpson GL, Blanchet FG, Kindt R, Legendre P, Minchin PR, et al. vegan: Community Ecology Package [Internet]. 2022. Available from: <https://CRAN.R-project.org/package=vegan>
53. Zhang X, Yi N. NBZIMM: negative binomial and zero-inflated mixed models, with application to microbiome/metagenomics data analysis. *BMC Bioinformatics.* 2020 Oct 30;21(1):488.
54. Zhang X, Mallick H, Tang Z, Zhang L, Cui X, Benson AK, et al. Negative binomial mixed models for analyzing microbiome count data. *BMC Bioinformatics.* 2017 Jan 3;18(1):4.
55. Ryu MH, Soumana IH, Wooding DJ, Leitao Filho FS, Yang J, Nislow C, et al. Relationship between Airway Microbiome and the Immune Response to Diesel Exhaust: A Randomized Crossover Controlled Exposure Study. *Environ Health Perspect.* 2024 Jul;132(7):077701.

56. Swiston JR, Davidson W, Attridge S, Li GT, Brauer M, Eeden SF van. Wood smoke exposure induces a pulmonary and systemic inflammatory response in firefighters. *Eur Respir J.* 2008 Jul 1;32(1):129–38.
57. Schwartz C, Bølling AK, Carlsten C. Controlled human exposures to wood smoke: a synthesis of the evidence. *Part Fibre Toxicol.* 2020 Oct 2;17(1):49.
58. Chen YW, Huang MZ, Chen CL, Kuo CY, Yang CY, Chiang-Ni C, et al. PM2.5 impairs macrophage functions to exacerbate pneumococcus-induced pulmonary pathogenesis. *Part Fibre Toxicol.* 2020 Aug 4;17:37.
59. Franzi LM, Bratt JM, Williams KM, Last JA. Why is particulate matter produced by wildfires toxic to lung macrophages? *Toxicol Appl Pharmacol.* 2011 Dec 1;257(2):182–8.
60. Ramos C, Cañedo-Mondragón R, Becerril C, González-Ávila G, Esquivel AL, Torres-Machorro AL, et al. Short-Term Exposure to Wood Smoke Increases the Expression of Pro-Inflammatory Cytokines, Gelatinases, and TIMPs in Guinea Pigs. *Toxics.* 2021 Sep 20;9(9):227.
61. Faas M, Ipseiz N, Ackermann J, Culemann S, Grüneboom A, Schröder F, et al. IL-33-induced metabolic reprogramming controls the differentiation of alternatively activated macrophages and the resolution of inflammation. *Immunity.* 2021 Nov 9;54(11):2531-2546.e5.
62. Buford M, Lacher S, Slattery M, Leving DC, Postma B, Holian A, et al. A mouse model of wildfire smoke-induced health effects: sex differences in acute and sustained effects of inhalation exposures. *Inhal Toxicol.* 2024 May 20;0(0):1–11.
63. Rylance J, Kankwatira A, Nelson DE, Toh E, Day RB, Lin H, et al. Household air pollution and the lung microbiome of healthy adults in Malawi: a cross-sectional study. *BMC Microbiol.* 2016 Aug 11;16(1):182.
64. Fitch MN, Phillipi D, Zhang Y, Lucero J, Pandey RS, Liu J, et al. Effects of Inhaled Air Pollution on Markers of Integrity, Inflammation, and Microbiota Profiles of the Intestines in Apolipoprotein E Knockout Mice. *Environ Res.* 2020 Feb;181:108913.
65. Mazumder MHH, Gandhi J, Majumder N, Wang L, Cumming RI, Stradtman S, et al. Lung-gut axis of microbiome alterations following co-exposure to ultrafine carbon black and ozone. *Part Fibre Toxicol.* 2023 Apr 21;20(1):15.
66. Segal LN, Alekseyenko AV, Clemente JC, Kulkarni R, Wu B, Chen H, et al. Enrichment of lung microbiome with supraglottic taxa is associated with increased pulmonary inflammation. *Microbiome.* 2013 Jul 1;1(1):19.
67. Durack J, Huang YJ, Nariya S, Christian LS, Ansel KM, Beigelman A, et al. Bacterial biogeography of adult airways in atopic asthma. *Microbiome.* 2018 Jun 9;6(1):104.
68. Sulaiman I, Wu BG, Li Y, Scott AS, Malecha P, Scaglione B, et al. Evaluation of the airway microbiome in nontuberculous mycobacteria disease. *Eur Respir J.* 2018 Oct;52(4):1800810.
69. Bingula R, Filaire E, Molnar I, Delmas E, Berthon JY, Vasson MP, et al. Characterisation of microbiota in saliva, bronchoalveolar lavage fluid, non-malignant, peritumoural and tumour tissue in

- non-small cell lung cancer patients: a cross-sectional clinical trial. *Respir Res.* 2020 May 25;21(1):129.
70. Leitao Filho FS, Monica Peters C, Sheel AW, Yang J, Nislow C, Lam S, et al. Characterization of the Lower Airways and Oral Microbiota in Healthy Young Persons in the Community. *Biomedicines.* 2023 Mar 10;11(3):841.
 71. Khemwong T, Kobayashi H, Ikeda Y, Matsuura T, Sudo T, Kano C, et al. *Fretibacterium* sp. human oral taxon 360 is a novel biomarker for periodontitis screening in the Japanese population. *PLoS ONE.* 2019 Jun 19;14(6):e0218266.
 72. Liu S, Xie G, Chen M, He Y, Yu W, Chen X, et al. Oral microbial dysbiosis in patients with periodontitis and chronic obstructive pulmonary disease. *Front Cell Infect Microbiol [Internet].* 2023 Feb 9 [cited 2024 May 27];13. Available from: <https://www.frontiersin.org/articles/10.3389/fcimb.2023.1121399>
 73. Bertelsen RJ, Barrionuevo AMP, Shigdel R, Lie SA, Lin H, Real FG, et al. Association of oral bacteria with oral hygiene habits and self-reported gingival bleeding. *J Clin Periodontol.* 2022 Aug;49(8):768–81.
 74. Agarwal DM, Dhotre DP, Kumbhare SV, Gaike AH, Brashier BB, Shouche YS, et al. Disruptions in oral and nasal microbiota in biomass and tobacco smoke associated chronic obstructive pulmonary disease. *Arch Microbiol.* 2021 Jul 1;203(5):2087–99.
 75. Pust MM, Tümmler B. Bacterial low-abundant taxa are key determinants of a healthy airway metagenome in the early years of human life. *Comput Struct Biotechnol J.* 2022 Jan 1;20:175–86.
 76. Han G, Luong H, Vaishnava S. Low abundance members of the gut microbiome exhibit high immunogenicity. *Gut Microbes.* 2022 Dec 31;14(1):2104086.
 77. Adam M. Does periodontitis affect respiratory health? *Evid Based Dent.* 2023 Sep;24(3):102–3.
 78. Kelly N, Winning L, Irwin C, Lundy FT, Linden D, McGarvey L, et al. Periodontal status and chronic obstructive pulmonary disease (COPD) exacerbations: a systematic review. *BMC Oral Health.* 2021 Sep 3;21(1):425.
 79. Lopes MP, Cruz ÁA, Xavier MT, Stöcker A, Carvalho-Filho P, Miranda PM, et al. *Prevotella intermedia* and periodontitis are associated with severe asthma. *J Periodontol.* 2020;91(1):46–54.
 80. Morris A, Beck JM, Schloss PD, Campbell TB, Crothers K, Curtis JL, et al. Comparison of the Respiratory Microbiome in Healthy Nonsmokers and Smokers. *Am J Respir Crit Care Med.* 2013 May 15;187(10):1067–75.

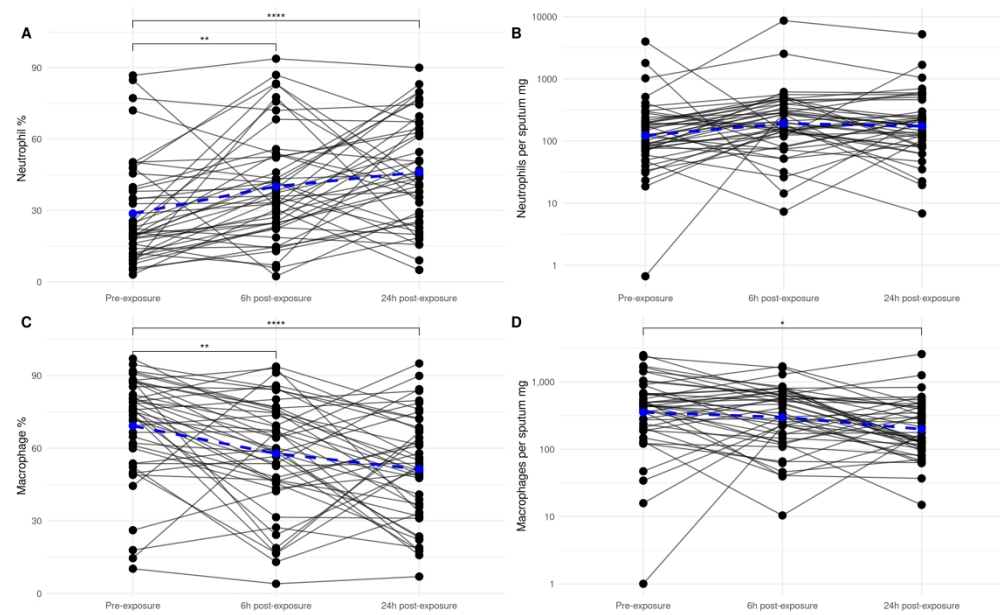


Figure 1

839x516mm (118 x 118 DPI)

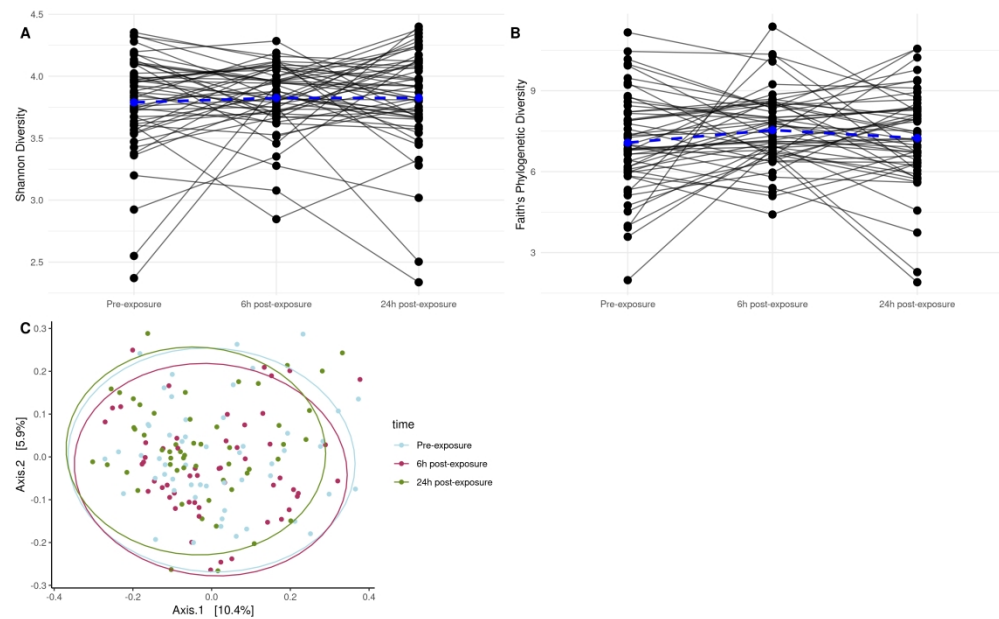


Figure 2

839x516mm (118 x 118 DPI)

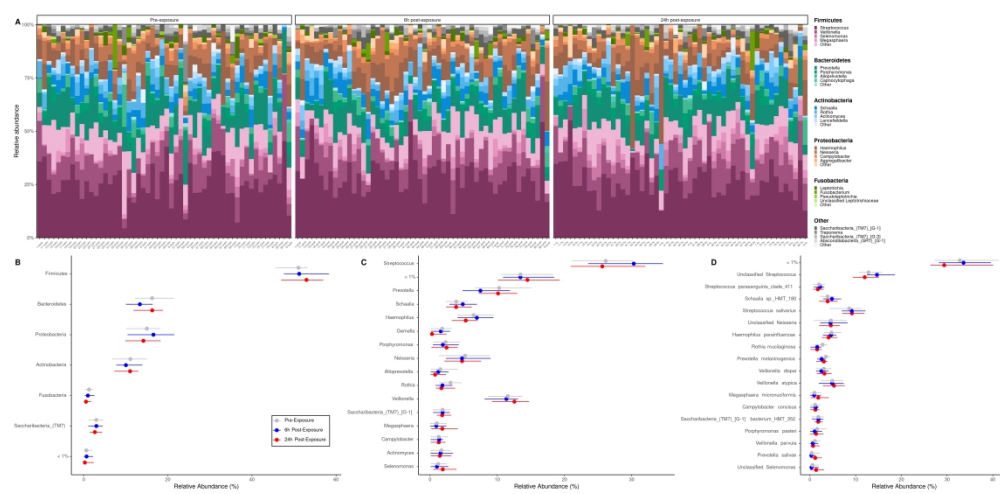


Figure 3

1614x774mm (118 x 118 DPI)

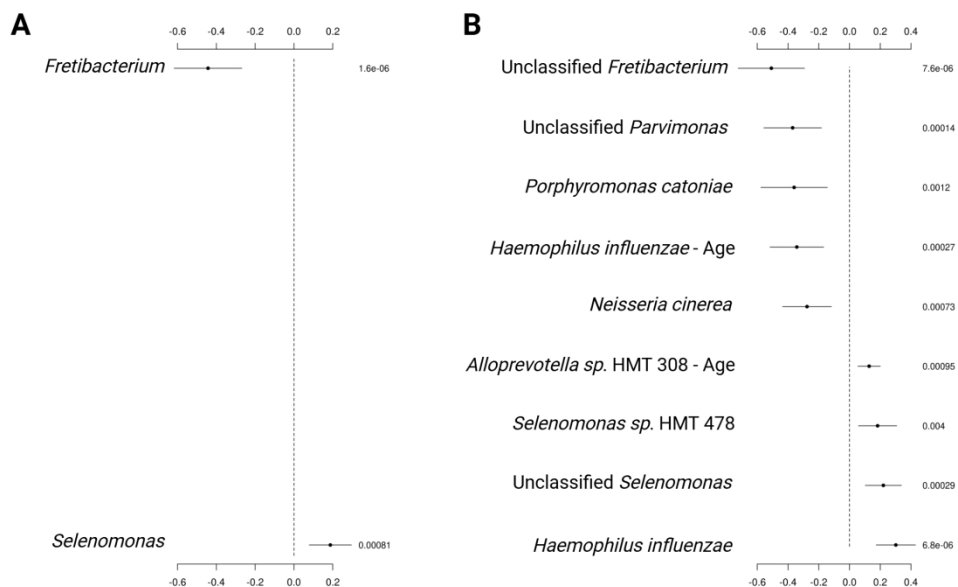


Figure 4

481x362mm (118 x 118 DPI)

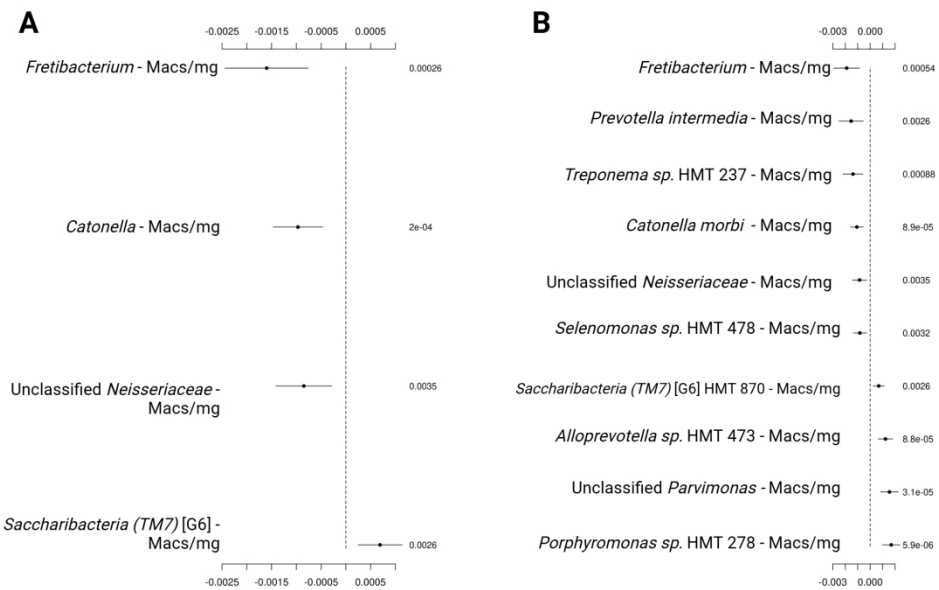


Figure 5

481x362mm (118 x 118 DPI)

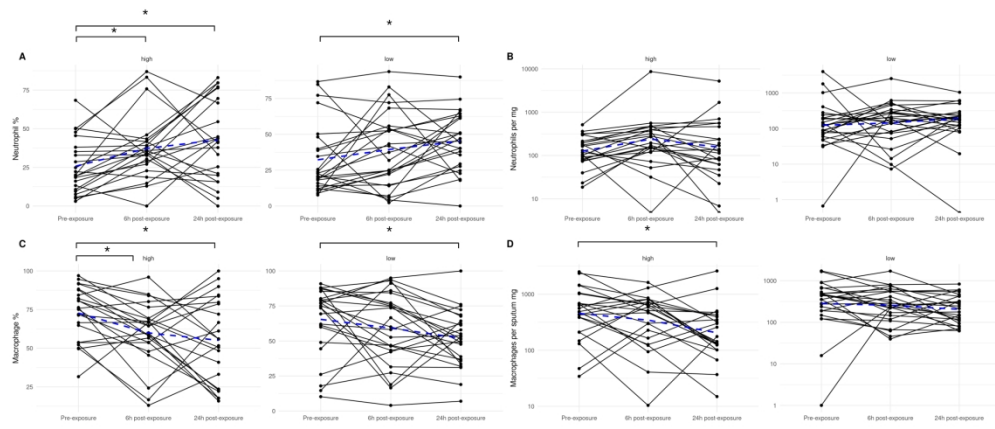


Figure 6

645x452mm (118 x 118 DPI)

Human Sputum Microbiome Composition and Sputum Inflammatory Cell Profiles Are Altered with Controlled Wood Smoke Exposure as a Model for Wildfire Smoke

Catalina Cobos-Uribe, MS - <https://orcid.org/0000-0002-6671-0780>, Radhika Dhingra, PhD - <http://orcid.org/0000-0003-0202-1860>, Martha A. Almond, Neil E. Alexis, MHSc, PhD - <https://orcid.org/0000-0002-9417-8269>, David B. Peden, MD, MS - <https://orcid.org/0000-0003-4526-4627>, Jeffrey Roach, PhD <https://orcid.org/0000-0001-9817-5877>, Meghan E. Reboli, PhD - <https://orcid.org/0000-0003-1918-2257>

ONLINE DATA SUPPLEMENT

Methods

Study participants

The population analyzed in this study (N=54, Table 1) constitutes a subset of participants from the SmokeScreen clinical study (NCT02767973). Detailed inclusion and exclusion criteria were previously described (1). In brief, exclusion criteria for this study were smoking, antibiotic use within four weeks of wood smoke exposure, pregnancy, symptomatic allergic rhinitis or active allergies, upper respiratory infection within four weeks of the challenge, presence of contraindicated or interfering medical conditions, and medication use that may impact response to wood smoke exposure (e.g., steroids, beta-agonists, and immunosuppressive drugs). Participants with mild asthma on controller therapy were asked to withhold this therapy for two weeks before wood smoke exposure. Only samples with sufficient induced sputum volume for downstream microbiome analysis were included in this study. This study was approved by the University of North Carolina Institutional Review Board (UNC IRB Numbers: 05-2528 and 15-1775).

Controlled exposure to wood smoke

Participants were exposed to 500 µg/m³ of wood smoke for two hours under controlled conditions at the U.S. EPA Human Studies Facility on the UNC-Chapel Hill campus from June 2016 to November 2022. Wood smoke was obtained by smoldering dried, untreated red oak logs. Generated smoke was injected into a human exposure chamber maintained at 22 °C and 40% humidity, as described by (2). To maximize wood smoke inhalation, participants were instructed to alternate between 15 minutes of exercise and 15 minutes of rest throughout the two-hour exposure period.

Induced sputum collection and processing

Induced sputum was collected and processed following the protocol outlined (3). Of note, participants rinsed their mouths and cleared their throats through gargling water prior to sputum induction to reduce potential oral contamination. Baseline samples were collected at a screening visit at least 24 hours prior to the wood smoke exposure visit, followed by collections at six- and 24 hours post-exposure (hpe). Following collection, samples were promptly transported on ice to the laboratory and processed. Briefly, plug selection was applied to the raw sputum samples. Then, samples were washed with DPBS Dulbecco's Phosphate-Buffered Saline (DPBS, Gibco, ThermoFisher Scientific, Cat# 14190144) and centrifuged. The supernatant was recovered and stored (-80 °C). Dithiothreitol (DTT, Sputolysin, EMD Millipore, CAS 578517) was used to treat the remaining cell mixture (15 minutes), followed by filtration to remove squamous cells, centrifugation, and recovery of DTT-supernatants and a cell pellet for hemocytometry evaluation and cytospin generation. DTT-treated supernatants were collected, aliquoted, and stored at -80°C. Sputum supernatants remained frozen until analysis. Samples containing fewer than 40% squamous cells were deemed to meet sputum quality control criteria. As only samples meeting quality

control criteria were stored in the biorepository utilized to generate the data in this study, all samples included in this study had already passed this quality control step by the biorepository, and no exclusions for sputum quality were necessary.

Markers of respiratory inflammatory response to wood smoke exposure

Total cell counts were determined from the sputum cell fraction using a Neubauer hematocytometer and Trypan Blue staining. Differential leukocyte analysis was performed on stained (Hema 3 stain) cytopsin slides, and counts were expressed as a percentage of total non-squamous nucleated cells and as cells per sputum mg. The sputum cytokine profile (IL-1 β , IL-6, IL-8, and TNF α) was determined from the DPBS treated sputum supernatant using a multiplex ELISA (MesoScale Discovery, Rockville, MD).

DNA extraction and 16S rRNA gene amplification and sequencing

Total DNA was extracted from the DTT-treated sputum supernatants. Mock sputum samples (n=3) and DNA extraction controls (n=7) were used as negative controls to identify possible contamination during sample processing. Mock samples were generated by subjecting sterile saline solutions (DPBS, Gibco, ThermoFisher Scientific, Cat# 14190144) to the sputum processing as described above and DNA extraction processing, followed by library preparation. Extraction controls consisted of sterile distilled ultrapure water aliquots, which were subjected to the same DNA extraction and library preparation protocol as the experimental samples. DNA extraction was completed using the DNeasy PowerSoil Pro kit (Qiagen, Germany) with a few modifications to the manufacturer's instructions. To process as much of the sample as possible, we used two PowerBead Pro tubes per sample and added 500-800 μ L of sample and 800 μ L of CD1 solution to each bead tube. Then, after vortexing and centrifuging, we transferred the entire supernatant to a clean microtube and added 400 μ L of CD2 solution, double the amount specified in the kit's instructions, to compensate for the larger supernatant volume. After centrifuging, we processed the entire supernatant solution (up to 700 μ L at a time) as indicated in the instructions using the same spin column until all the solution was transferred. After this point, we followed the instructions provided by the manufacturer until the final elution step, where the extracted DNA was eluted to a final volume of 30 μ L. DNA was quantified with the QubitTM Flex Fluorometer and the QubitTM dsDNA Broad Range Quantitation kit (ThermoFisher Scientific, USA) using 5 μ L aliquots. The extracted DNA was stored at -80 °C until sequencing. Extracted DNA was sent to SeqCenter (SeqCenter LLC, PA, USA) for amplification and high-throughput sequencing. Samples were prepared using the Quick-16STM NGS Library Prep Kit (Zymo Research, USA) with phased primers targeting the V3-V4 region of the 16S rRNA gene (Forward sequences: CCTACGGGDGGCWGCAG and CCTAYGGGGYGCWGCAG; Reverse sequence: GACTACHVGGGTATCTAATCC). Samples were sequenced on a P1 600cyc NextSeq 2000 Flowcell, producing 2x301 bp paired-end reads.

Bioinformatic analysis

Raw sequencing data were converted to the FASTQ format and demultiplexed with bcl-convert (4). These sequences were imported into QIIME2 (5), where primer sequences were removed using the Cutadapt plugin (6). Sequences were denoised using the dada2 plugin (7). Denoised sequences were assigned taxonomic identifiers using two databases: the commonly used SILVA database (8) and the extended Human Oral Microbiome Database (eHOMD) (9), which focuses on bacteria in the human aerodigestive tract; thus, enhancing taxonomic classification resolution. Hereafter, eHOMD is included in the main body of this paper, and SILVA is in the supplemental material. Finally, the metadata, phylogenetic tree, and feature and taxa tables were imported into RStudio using the *qiime2R* R package (version 0.99.6) (10) and used to create a phyloseq object (*phyloseq* package version 1.38.0). The *decontam* package (version 1.14.0) (11) was used to identify and remove contaminant sequences in our data, using mock sputum samples and extraction controls as negative controls ($n = 10$), using the prevalence method with a 0.1 threshold. Seventeen contaminant sequences were identified and removed from the phyloseq object. Contaminant sequences and their relative abundance and prevalence in sputum samples are reported in Supplementary Tables E1 and 2). This and all subsequent analyses and visualizations were carried out using R version 4.1.0 (12) in RStudio (13).

Data analysis

Host respiratory inflammatory response: Inflammatory cell and cytokine production data were analyzed using a repeated measures one-way ANOVA followed by pairwise paired *t*-tests to assess the statistical significance between the exposure times (aggregate analysis). For stratified analysis by sex, a repeated measures two-way ANOVA was used, followed by pairwise *t*-tests for comparison between treatment groups and between time points. Based on Q-Q plot assessments of normality (Supplemental Figure 1), percentage macrophage and neutrophil data were approximately normal and thus run via parametric tests. Subjects with missing inflammatory cell or cytokine data were excluded from the analysis, resulting in a final dataset of 45 subjects for inflammatory cell analysis (30 females, 15 males) and 35 subjects for cytokine analysis (20 females, 15 males). Absolute cell counts and cytokine data were log-transformed to more closely align with normal distribution.

Microbiome diversity: Alpha diversity metrics were determined using two different R packages. Shannon index was estimated with the *estimate_richness* function in *phyloseq* (14) and Faith's phylogenetic diversity was calculated with the *estimate_pd* function in *btools* (15). For statistical analysis, we used the same approach as with the host immune response with data log transformation to better align the associated Q-Q plots (Supplemental Figure 1). Beta diversity (Bray-Curtis dissimilarity) was calculated using the *adonis2* function from the *vegan* package (version 2.6-4) (16); results were visualized using a principal coordinate

analysis (PCoA). Beta diversity was evaluated between exposure groups with and without metadata variables (e.g. sex). To assess the impact of exposure and other factors on beta diversity, we employed a Permutation Multivariate Analysis of Variance (PERMANOVA). PERMANOVA was chosen for beta diversity and differs from the tests used for alpha diversity and inflammatory responses above and to account for the non-independence of samples within subjects, as the Bray-Curtis dissimilarity index is a distance matrix to control for within-subject variability, thus these data points lack the independence required by the assumptions of a one-way ANOVA. Given the repeated measures design of our study, we incorporated the ‘strata’ argument in our *adonis2* analysis to account for the non-independence of samples within subjects, thereby controlling for within-subject variability and preventing pseudoreplication.

Differential abundance analysis and host-microbiome associations: Relative abundance bar plots were created using the *microshades* package (17). To facilitate the visualization of relative abundance, we created plots at the phylum, genus, and species taxonomic levels. Differential abundance analysis was performed with a negative binomial mixed model (NBMM) controlling for age, sex, BMI, and asthma status using the *nlme* and *NBZIMM* packages and a minimum prevalence of 20% (18). Other demographic factors were assessed as sensitivity analyses in the model, but did not substantially alter the results (Supplementary Tables E6X, 8, 10, and 12). This model is recommended for longitudinal microbiome data because it accounts for the over-dispersion and sparsity present in microbiome count data while also handling the repeated measures from the same subject over time (i.e., random effect = subject), improving the reliability of statistical inferences about microbial abundance changes and the effects of covariates (18,19). Finally, using the same NBMM model, we explored potential host-microbiome associations by including immune cell data as model covariates. To investigate potential host-microbiome associations between sputum macrophages and microbiome taxa, we applied the same NBMM model, including macrophage per sputum mg data as a model covariates. Additionally, we performed a stratified analysis to examine host-microbiome associations further (54). This analysis compared cytokine and inflammatory cell data between groups defined by baseline microbiome observed richness. Richness groups were classified as high or low based on the study median (median ASV = 126). The low-richness group included samples with ASV <126, while the high-richness group included samples with ASV >126.

All *p*-values were corrected for multiple comparisons using the Benjamin-Hochberg false discovery rate (FDR) correction. Reported *p*-values throughout the manuscript are adjusted unless otherwise specified. For repeated measures one-way ANOVA, FDR correction was applied separately to each analysis set. For inflammatory cell analyses, FDR correction accounted for four comparisons (one per variable across three timepoints); for alpha diversity, two comparisons (one per diversity metric across three timepoints). For

the differential abundance analysis using a NBMM, FDR correction was applied to 170 comparisons at the genus level and 450 at the species level, corresponding to the number of taxa analyzed.

Supplementary Figure Legends

Supplementary Figure E1. Q-Q plots for macrophage and neutrophil percentages and absolute values, inflammatory cytokines (IL-1 beta, IL-6, IL-8, and TNF alpha), and alpha diversity measures (Shannon and Faith PD) at each timepoint (Pre-Exposure, 6 hours post-exposure, and 24 hours post-exposure). The plots assess the normality of the data distribution across the different variables and timepoints.

Supplementary Figure E2. Total cells per sputum mg observed following wood smoke exposure. Total cell counts were performed Pre-exposure, at six hours post-exposure, and at 24 hours post-exposure. Data is presented as individual data points connected by lines to represent paired analysis for each subject. The blue dashed line represents the mean. Analyzed with repeated measures one-way ANOVA.

Supplementary Figure E3. Sputum inflammatory cell host response following wood smoke exposure analyzed by sex. Induced sputum cell differentials were stained and counted for neutrophils and macrophages prior to exposure (Pre-exposure), at six hours post-exposure (6h post-exposure), and at 24 hours post-exposure (24h post-exposure). A) Relative percentage of neutrophils, B) absolute neutrophils per mg of sputum, C) relative percentage of macrophages, and D) absolute macrophages per mg of sputum are shown in box and whisker plots. Analyzed with repeated measures two-way ANOVA followed by pairwise paired t-tests. Purple (left) = females; Blue (right) = males. P-values shown (* $P \leq 0.05$, ** $P \leq 0.01$, and *** $P \leq 0.0001$) correspond to the paired t-test results. Purple lines below significance * are representative of significant differences between females across exposure groups. Black lines below significance * are representative of sex differences within exposure groups.

Supplementary Figure E4. Sputum cytokine response following wood smoke exposure. Cytokine profiles were measured from DPBS-treated sputum supernatants prior to exposure (Pre-exposure), at six hours post-exposure (6h post-exposure), and at 24 hours post-exposure (24h post-exposure). A) Interleukin-1 β (IL-1 β), B) Interleukin-6 (IL-6), C) Interleukin-8 (IL-8), and D) Tumor Necrosis Factor- α (TNF- α). Analyzed with repeated measures one-way ANOVA followed by pairwise paired t-tests.

Supplementary Figure E5. Sputum cytokine response following wood smoke exposure analyzed by sex. Cytokine profiles were measured from DPBS-treated sputum supernatants prior to exposure (Pre-exposure), at six hours post-exposure (6h post-exposure), and at 24 hours post-exposure (24h post-exposure). A) Interleukin-1 β (IL-1 β), B) Interleukin-6 (IL-6), C) Interleukin-8 (IL-8), and D) Tumor Necrosis Factor- α (TNF- α). Analyzed with repeated measures one-way ANOVA followed by pairwise paired t-tests. Purple (left) = females; Blue (right) = males. P-values shown (* $P \leq 0.05$) correspond to the paired t-test results. Black lines below significance * are representative of sex differences within exposure groups.

Supplementary Figure E6. Sputum microbiome alpha diversity with exposure to wood smoke analyzed by sex. Induced sputum supernatants were analyzed via 16S rRNA sequencing. Samples prior to exposure (Pre-exposure), at six hours post-exposure (6h post-exposure), and 24 hours post-exposure (24h post-exposure) were evaluated for differences in alpha diversity. Alpha diversity was analyzed by Shannon's (A) and Faith's (B) indices. Purple (left) = females; Blue (right) = males.

Supplementary Figure E7. Principal Coordinates Analysis (PCoA) of beta diversity. Lines between data points connect the three data points for each subject to illustrate individual changes across time points. Panels B, C, and D display only two data points at a time to improve visualization.

Supplementary Figure E8. Sputum microbiome composition. Induced sputum supernatants from study participants exposed to wood smoke were collected pre-exposure, 6 h post-exposure, and 24 h post-exposure. Samples were analyzed via 16S rRNA sequencing and annotated using SILVA. (A) Microbiome composition by relative abundance at the genus level for individual participants. (B-D) Aggregate median relative abundances at the (B) phylum, (C) genus, and (D) species level. Error bars represent the interquartile range.

Supplementary Figure E9. Sputum microbiome differential abundance analysis for effects of wood smoke exposure at the (A) genus and (B) species level using SILVA and a negative binomial mixed model (NBMM) controlling for age, sex, BMI, and asthma status. Bacteria that were significantly affected by exposure are shown on the left of each plot, the direction and magnitude of effect shown in the middle of each plot, and the associated p-value on the right of each plot.

Supplementary Figure E10. Sputum cytokine response following wood smoke exposure stratified by baseline microbiome richness. Cytokine profiles were measured from DPBS-treated sputum supernatants prior to exposure (Pre-exposure), at six hours post-exposure (6h post-exposure), and at 24 hours post-exposure (24h post-exposure). A) Interleukin-1 β (IL-1 β), B) Interleukin-6 (IL-6), C) Interleukin-8 (IL-8), and D) Tumor Necrosis Factor- α (TNF- α). Analyzed with repeated measures one-way ANOVA followed by pairwise paired t-tests.

References

1. Alexis NE, Zhou LY, Burbank AJ, Almond M, Hernandez ML, Mills KH, et al. Development of a screening protocol to identify persons who are responsive to wood smoke particle-induced airway inflammation with pilot assessment of GSTM1 genotype and asthma status as response modifiers. *Inhal Toxicol.* 2022;34(11–12):329–39.
2. Ghio AJ, Soukup JM, Case M, Dailey LA, Richards J, Berntsen J, et al. Exposure to wood smoke particles produces inflammation in healthy volunteers. *Occup Environ Med.* 2012 Mar 1;69(3):170–5.
3. Alexis N, Soukup J, Ghio A, Becker S. Sputum Phagocytes from Healthy Individuals Are Functional and Activated: A Flow Cytometric Comparison with Cells in Bronchoalveolar Lavage and Peripheral Blood. *Clin Immunol.* 2000 Oct 1;97(1):21–32.
4. Illumina. BCL Convert: a proprietary Illumina software for the conversion of BCL files to basecalls. [Internet]. 2021 [cited 2023 Nov 21]. Available from: https://support-docs.illumina.com/SW/BCL_Convert/Content/SW/FrontPages/BCL_Convert.htm
5. Bolyen E, Rideout JR, Dillon MR, Bokulich NA, Abnet CC, Al-Ghalith GA, et al. Reproducible, interactive, scalable and extensible microbiome data science using QIIME 2. *Nat Biotechnol.* 2019 Aug;37(8):852–7.
6. Martin M. Cutadapt removes adapter sequences from high-throughput sequencing reads. *EMBnet.journal.* 2011 May 2;17(1):10–2.
7. Callahan BJ, McMurdie PJ, Rosen MJ, Han AW, Johnson AJA, Holmes SP. DADA2: High resolution sample inference from Illumina amplicon data. *Nat Methods.* 2016 Jul;13(7):581–3.
8. Quast C, Pruesse E, Yilmaz P, Gerken J, Schweer T, Yarza P, et al. The SILVA ribosomal RNA gene database project: improved data processing and web-based tools. *Nucleic Acids Res.* 2013 Jan 1;41(D1):D590–6.
9. Escapa IF, Chen T, Huang Y, Gajare P, Dewhirst FE, Lemon KP. New Insights into Human Nostril Microbiome from the Expanded Human Oral Microbiome Database (eHOMD): a Resource for the Microbiome of the Human Aerodigestive Tract. *mSystems.* 2018 Dec 4;3(6):e00187-18.
10. Bisanz JE. qiime2R: Importing QIIME2 artifacts and associated data into R sessions [Internet]. 2018 [cited 2024 Jun 18]. Available from: <https://github.com/jbisanz/qiime2R>
11. Davis NM, Proctor DM, Holmes SP, Relman DA, Callahan BJ. Simple statistical identification and removal of contaminant sequences in marker-gene and metagenomics data. *Microbiome.* 2018 Dec 17;6(1):226.
12. R Core Team. R: A Language and Environment for Statistical Computing [Internet]. Vienna, Austria: R Foundation for Statistical Computing; 2021. Available from: <https://www.R-project.org/>
13. Posit team. RStudio: Integrated Development Environment for R [Internet]. Boston, MA: Posit Software, PBC; 2023. Available from: <http://www.posit.co/>
14. McMurdie PJ, Holmes S. phyloseq: An R Package for Reproducible Interactive Analysis and Graphics of Microbiome Census Data. *PLOS ONE.* 2013 abr;8(4):e61217.

15. Battaglia, Thomas. GitHub. 2015 [cited 2024 Jun 18]. btools: A suite of R function for all types of microbial diversity analyses. Available from: <https://github.com/twbattaglia/btools/blob/master/README.md>
16. Oksanen J, Simpson GL, Blanchet FG, Kindt R, Legendre P, Minchin PR, et al. vegan: Community Ecology Package [Internet]. 2022. Available from: <https://CRAN.R-project.org/package=vegan>
17. Dahl EM, Neer E, Bowie KR, Leung ET, Karstens L. microshades: An R Package for Improving Color Accessibility and Organization of Microbiome Data. *Microbiol Resour Announc.* 2022;11(11):e00795-22.
18. Zhang X, Yi N. NBZIMM: negative binomial and zero-inflated mixed models, with application to microbiome/metagenomics data analysis. *BMC Bioinformatics.* 2020 Oct 30;21(1):488.
19. Zhang X, Mallick H, Tang Z, Zhang L, Cui X, Benson AK, et al. Negative binomial mixed models for analyzing microbiome count data. *BMC Bioinformatics.* 2017 Jan 3;18(1):4.

Supplementary Table E1. Contaminant Sequences Identified Using the Prevalence Method of the *decontam* R package

	Kingdom	Phylum	Class	Order	Family	Genus	Species
6dbcc01ebc2af8182d70663db558527	Bacteria	Proteobacteria	Betaproteobacteria	Burkholderiales	Burkholderiaceae	Burkholderia	cepacia
8c346b3fac6d07017ead998035914b88	Bacteria	Proteobacteria	Betaproteobacteria	Burkholderiales	Burkholderiaceae	Burkholderia	cepacia
5f8b99d96b9fb65e12c944b3f8bd38b9	Bacteria	Proteobacteria	Betaproteobacteria	Burkholderiales	Burkholderiaceae	Burkholderia	cepacia
ffc36e27c82042664a16bcd4d380b286	Bacteria	Proteobacteria	Gammaproteobacteria	Enterobacteriales	Enterobacteriaceae	Escherichia	coli
d55b64807e7fc58167f15fce10f0695c0	Bacteria	Proteobacteria	Alphaproteobacteria	Hyphomicrobiales	Brucellaceae	Brucella	anthropi
dd8c8d60bfcfa3e1d01a4bf8d3326e	Bacteria	Proteobacteria	Alphaproteobacteria	Sphingomonadales	Sphingomonadaceae	Sphingomonas	glacialis
89a04ae48354976f71d111d52a609e8	Bacteria	Proteobacteria	Alphaproteobacteria	Sphingomonadales	Sphingomonadaceae	Novosphingobium	humi
283be7225e0ecd411525948112368a2	Bacteria	Proteobacteria	Alphaproteobacteria	Sphingomonadales	Sphingomonadaceae	Novosphingobium	humi
9db2817f5c42be6a7bcbca662959982d	Bacteria	Proteobacteria	Alphaproteobacteria	Hyphomicrobiales	Bradyrhizobiaceae	NA	NA
7f94ba24ae3488c6a0fcbe0587b78c59	Bacteria	Proteobacteria	Alphaproteobacteria	Hyphomicrobiales	Bradyrhizobiaceae	NA	NA
455bb9658a6da2552eddb8e918b1472	Bacteria	Proteobacteria	Alphaproteobacteria	Hyphomicrobiales	Bradyrhizobiaceae	NA	NA
7507ee1be078be2cf7444825dcde58b25	Bacteria	Proteobacteria	Alphaproteobacteria	Caulobacterales	Caulobacteraceae	Brevundimonas	diminuta
2cd30e9eda91687ba73dcae76f4f1880	Bacteria	Proteobacteria	Alphaproteobacteria	Caulobacterales	Caulobacteraceae	Brevundimonas	diminuta
b02a8d3d018119deb2db15db887bfd	Bacteria	Actinobacteria	Actinomycetia	Propionibacteriales	Propionibacteriaceae	Cutibacterium	acnes
3c5f98e32cb2d4d18090f2d7f9f17015	Bacteria	Firmicutes	Clostridia	Eubacteriales	Peptostreptococcaceae	Peptostreptococcaceae[G5]	HMT493
3fe8608797c2760295ca61479f630cb6	Bacteria	Firmicutes	Clostridia	Eubacteriales	Peptostreptococcaceae	Mogibacterium	NA
5497318e515a8c328a68f957d9c7d4	Bacteria	Firmicutes	Bacilli	Bacillales	Staphylococcaceae	Staphylococcus	capitis

Supplementary Table E2. Relative Abundance and Prevalence of Contaminant Sequences in Negative Controls and True Sputum Samples

	Family	Genus	Species	Mean Relative Abundance (%)		Prevalence	
				Negative controls	Sputum samples	Negative controls	Sputum samples
283be7225e0ecd411525948112368a2	Sphingomonadaceae	Novosphingobium	humi	2.41105585	0	0.2	0
2cd30e9eda91687ba73dcae76f4f1880	Caulobacteraceae	Brevundimonas	diminuta	2.57331265	0	0.2	0
3c5f98e32eb2d4d18090f2d7f9f17015	Peptostreptococcaceae	Peptostreptococcaceae[G-5]	bacterium HMT493	0.94598605	0.002226525	0.1	0.00621118
3fe8608797c2760295ca61479f630cb6	Peptostreptococcaceae	Mogibacterium	NA	0.06083894	0.000701009	0.1	0.01242236
455bb9658a6da2552eddb8e918b1472	Bradyrhizobiaceae	NA	NA	0.21822894	0	0.2	0
5497318e515a8c328a68f957d9c7d4	Staphylococcaceae	Staphylococcus	capitis	0.52114865	0.001443256	0.1	0.01242236
5f8b99d96b9fb65e12c944b3f8bd38b9	Burkholderiaceae	Burkholderia	cepacia	0.40582216	0	0.2	0
6dbcc01ebc2af8182d70663db558527	Burkholderiaceae	Burkholderia	cepacia	5.67507778	0	0.3	0
7507ee1be078be2cf7444825dc58b25	Caulobacteraceae	Brevundimonas	diminuta	0.06648661	0	0.2	0
7f94ba24ae3488c6a0fcbe0587b78c59	Bradyrhizobiaceae	NA	NA	0.31810694	0	0.4	0
89a04ae48354976f71d111d52a609e8	Sphingomonadaceae	Novosphingobium	humi	0.23926992	0	0.2	0
8c346b3fac6d07017ead998035914b88	Burkholderiaceae	Burkholderia	cepacia	0.27966056	0	0.2	0
9db2817f5c42be6a7bcbca662959982d	Bradyrhizobiaceae	NA	NA	3.44972578	0	0.4	0
b02a8d3d018119deb2db15db887bfd	Propionibacteriaceae	Cutibacterium	acnes	3.66583601	0	0.4	0
d55b64807e7fc58167f15ce10f0695c0	Brucellaceae	Brucella	anthropi	1.32335596	0	0.2	0
dd8c8d60bfcfa3e1d01a4bf8d3326e	Sphingomonadaceae	Sphingomonas	glacialis	5.9653503	0	0.4	0
ffc36e27c82042664a16bcd4d380b286	Enterobacteriaceae	Escherichia	coli	1.90998961	0	0.3	0

Supplementary Table E3. Beta Diversity PERMANOVA Results

	Df	SumOfSqs	R2	F	Pr(>F)
Exposure (hpe)	2	0.388	0.01024	0.817	0.001
Residual	158	37.480	0.98976		
Total	160	37.868	1		

Supplementary Table E4. Beta Diversity PERMANOVA Results by Exposure and Sex

	Df	SumOfSqs	R2	F	Pr(>F)
Exposure (hpe)	2	0.388	0.01024	0.8195	0.002
Sex	1	0.589	0.01554	2.4890	0.005
Exposure: Sex	2	0.234	0.00618	0.4951	0.584
Residual	155	36.658	0.96803		
Total	160	37.868	1		

Supplementary Table E5. Negative Binomial Mixed Model Results for Genus-Level Microbiome Differential Abundance Analysis Using eHOMD

	Estimate	Std.Error	p-value	p-adj	Exp.Estimate	Percent Change	Increase/Decrease
<i>Fretibacterium</i>	-0.442817	0.0872207	1.65 x 10-06	6.76 x 10-05	0.642224723	35.78	↓
<i>Selenomonas</i>	0.1875918	0.0543699	8.05 x 10-04	1.65 x 10-02	1.206340986	20.63	↑

Supplementary Table E6. Negative Binomial Mixed Model Results for Genus-Level Microbiome Differential Abundance Analysis Using eHOMD and Incorporating Race as a Covariate

	Estimate	Std.Error	p-value	p-adj	Exp.Estimate	Percent Change	Increase/Decrease
<i>Fretibacterium</i>	-0.4419975	0.0882453	2.20 x 10-06	9.01 x 10-05	0.642751242	35.72	↓
<i>Selenomonas</i>	0.1870556	0.0550483	9.57 x 10-04	1.96 x 10-02	1.20569432	20.57	↑

Supplementary Table E7. Negative Binomial Mixed Model Results for Species-Level Microbiome Differential Abundance Analysis Using eHOMD

	Estimate	Std.Error	p-value	p-adj	Exp.Estimate	Percent Change	Increase/Decrease
Unclassified <i>Fretibacterium</i>	-0.5081605	0.1078981	7.56 x 10-06	0.0003212	0.601601207	39.84	↓
Unclassified <i>Parvimonas</i>	-0.3697333	0.0935324	1.40 x 10-04	0.0039531	0.690918574	30.91	↓
<i>Porphyromonas catoniae</i>	-0.3601067	0.1080873	1.19 x 10-03	0.0168479	0.697601888	30.24	↓
<i>Haemophilus influenzae</i>-Age	-0.3426197	0.0872579	2.69 x 10-04	0.0229021	0.709908138	29.01	↓
<i>Neisseria cinerea</i>	-0.2761827	0.079379	7.31 x 10-04	0.0124233	0.758674308	24.13	↓
<i>Alloprevotella</i> sp. HMT 308-Age	0.1275712	0.0362543	9.46 x 10-04	0.0402247	1.136065753	13.61	↑
<i>Selenomonas</i> sp. HMT 478	0.1827091	0.0621528	4.03 x 10-03	0.0489787	1.200465142	20.05	↑
Unclassified <i>Selenomonas</i>	0.2200454	0.0587238	2.91 x 10-04	0.006194	1.246133304	24.61	↑
<i>Haemophilus influenzae</i>	0.3013354	0.0636323	6.80 x 10-06	0.0003212	1.351662613	35.17	↑

Supplementary Table E8. Negative Binomial Mixed Model Results for Species-Level Microbiome Differential Abundance Analysis Using eHOMD and Incorporating Race as a Covariate

	Estimate	Std.Error	p-value	p-adj	Exp.Estimate	Percent Change	Increase/ Decrease
Unclassified <i>Fretibacterium</i>	-0.507625	0.108974	9.30 x 10-06	7.81 x 10-04	0.60192327	39.81	↓
<i>Haemophilus influenzae</i>-Age	-0.421349	0.07417	8.69 x 10-07	7.30 x 10-05	0.656161389	34.38	↓
Unclassified <i>Parvimonas</i>	-0.371045	0.094455	1.53 x 10-04	6.41 x 10-03	0.690013097	31.00	↓
<i>Porphyromonas catoniae</i>	-0.36099	0.108453	1.20 x 10-03	2.02 x 10-02	0.696985829	30.30	↓
<i>Neisseria cinerea</i>	-0.278123	0.080444	7.86 x 10-04	1.65 x 10-02	0.757203831	24.28	↓
Unclassified <i>Selenomonas</i>	0.220623	0.058271	2.54 x 10-04	7.11 x 10-03	1.24685278	24.69	↑
<i>Haemophilus influenzae</i>-BMI	0.31028	0.076839	2.02 x 10-04	1.70 x 10-02	1.363806517	36.38	↑

Supplementary Table E9. Negative Binomial Mixed Model Results for Genus-Level Host-Microbiome Association Analysis Using eHOMD

	Variable	Estimate	Std.Error	p-value	p-adj	Exp Estimate	Percent Change	Increase/ Decrease
<i>Fretibacterium</i>	Exposure (hpe)	-0.55138	0.088516	1.31 x 10-08	5.37 x 10-07	0.576152	42.38	↓
<i>Fretibacterium</i>	Macrophages/mg	-0.0016	0.000421	2.60 x 10-04	5.34 x 10-03	0.998402	0.16	↓
<i>Catonella</i>	Macrophages/mg	-0.00097	0.00025	2.02 x 10-04	5.34 x 10-03	0.999033	0.10	↓
Unclassified <i>Neisseriaceae</i>	Macrophages/mg	-0.00085	0.000283	3.52 x 10-03	3.61 x 10-02	0.999152	0.08	↓
<i>Saccharibacteria (TM7) [G-6]</i>	Macrophages/mg	0.00069	0.000223	2.59 x 10-03	3.54 x 10-02	1.000691	0.07	↑

Supplementary Table E10. Negative Binomial Mixed Model Results for Genus-Level Host-Microbiome Association Analysis Using eHOMD and Incorporating Race as a Covariate

	Variable	Estimate	Std.Error	p-value	p-adj	Exp Estimate	Percent Change	Increase/ Decrease
<i>Fretibacterium</i>	Exposure (hpe)	-0.55325	0.090658	2.32 x 10-08	9.26 x 10-07	0.575076	42.49	↓
<i>Fretibacterium</i>	Macrophages/mg	-0.00164	0.00043	2.48 x 10-04	4.95 x 10-03	0.998363	0.16	↓
<i>Catonella</i>	Macrophages/mg	-0.00097	0.000251	2.15 x 10-04	4.95 x 10-03	0.999033	0.10	↓
Unclassified <i>Neisseriaceae</i>	Macrophages/mg	-0.00086	0.000286	3.36 x 10-03	4.48 x 10-02	0.99914	0.09	↓

Supplementary Table E11. Negative Binomial Mixed Model Results for Species-Level Host-Microbiome Association Analysis using eHOMD

	Variable	Estimate	Std.Error	p-value	p-adj	Exp.Estimate	Percent Change	Increase/Decrease
Unclassified <i>Fretibacterium</i>	Exposure (hpe)	-0.66859	0.111931	4.12 x 10-08	3.59 x 10-06	0.512431	48.76	↓
<i>Campylobacter rectus</i>	Exposure (hpe)	-0.49926	0.142113	6.83 x 10-04	1.51 x 10-02	0.606982	39.30	↓
<i>Prevotella intermedia</i>	Exposure (hpe)	-0.45469	0.133728	9.90 x 10-04	1.51 x 10-02	0.634647	36.54	↓
<i>Haemophilus influenzae</i>	Age	-0.36084	0.08969	2.28 x 10-04	1.23 x 10-02	0.697092	30.29	↓
<i>Haemophilus sp. HMT 908</i>	Exposure (hpe)	-0.33559	0.099066	1.03 x 10-03	1.51 x 10-02	0.714913	28.51	↓
<i>Neisseria cinerea</i>	Exposure (hpe)	-0.28815	0.085118	1.04 x 10-03	1.51 x 10-02	0.749649	25.04	↓
Unclassified <i>Fretibacterium</i>	Macrophages/mg	-0.00189	0.000526	5.36 x 10-04	9.32 x 10-03	0.998114	0.19	↓
<i>Prevotella intermedia</i>	Macrophages/mg	-0.00153	0.000493	2.58 x 10-03	2.81 x 10-02	0.998474	0.15	↓
<i>Treponema sp. HMT 237</i>	Macrophages/mg	-0.00137	0.000399	8.79 x 10-04	1.27 x 10-02	0.998628	0.14	↓
<i>Cattonella morbi</i>	Macrophages/mg	-0.00107	0.000261	8.89 x 10-05	1.93 x 10-03	0.998932	0.11	↓
Unclassified <i>Neisseriaceae</i>	Macrophages/mg	-0.00085	0.000283	3.52 x 10-03	3.06 x 10-02	0.999152	0.08	↓
<i>Selenomonas sp. HMT 478</i>	Macrophages/mg	-0.00082	0.000272	3.20 x 10-03	3.06 x 10-02	0.999176	0.08	↓
<i>Saccharibacteria (TM7) [G6] HMT 870</i>	Macrophages/mg	0.00069	0.000223	2.59 x 10-03	2.81 x 10-02	1.000691	0.07	↑
<i>Alloprevotella sp. HMT 473</i>	Macrophages/mg	0.001229	0.0003	8.77 x 10-05	1.93 x 10-03	1.00123	0.12	↑
Unclassified <i>Parvimonas</i>	Macrophages/mg	0.001553	0.000355	3.07 x 10-05	1.34 x 10-03	1.001554	0.16	↑
<i>Porphyromonas sp. HMT 278</i>	Macrophages/mg	0.001696	0.000353	5.91 x 10-06	5.14 x 10-04	1.001697	0.17	↑
<i>Alloprevotella sp. HMT 308</i>	Age	0.143162	0.04193	1.41 x 10-03	4.08 x 10-02	1.153917	15.39	↑
<i>Stomatobaculum longum</i>	Age	0.161942	0.040968	2.83 x 10-04	1.23 x 10-02	1.175792	17.58	↑
Unclassified <i>Selenomonas</i>	Exposure (hpe)	0.236566	0.072645	1.57 x 10-03	1.95 x 10-02	1.266891	26.69	↑
<i>Haemophilus influenzae</i>	Exposure (hpe)	0.401574	0.078013	1.44 x 10-06	6.28 x 10-05	1.494174	49.42	↑

Supplementary Table E12. Negative Binomial Mixed Model Results for Species-Level Host-Microbiome Association Analysis using eHOMD and Incorporating Race as a Covariate

	Variable	Estimate	Std.Error	p-value	p-adj	Exp.Estimate	Percent Change	Increase/Decrease
<i>Alloprevotella sp. HMT 308</i>	Sex (Male)	-3.02855	0.439122	2.61 x 10-08	2.06 x 10-06	0.048386	95.16	↓
<i>Streptococcus parasanguinis clade 411</i>	Sex (Male)	-0.80719	0.238385	1.60 x 10-03	4.46 x 10-02	0.44611	55.39	↓
Unclassified <i>Fretibacterium</i>	Exposure (hpe)	-0.67436	0.114705	6.26 x 10-08	4.94 x 10-06	0.509481	49.05	↓
<i>Campylobacter rectus</i>	Exposure (hpe)	-0.50725	0.143344	6.27 x 10-04	2.16 x 10-02	0.602151	39.78	↓
<i>Prevotella intermedia</i>	Exposure (hpe)	-0.45061	0.134675	1.18 x 10-03	2.16 x 10-02	0.637241	36.28	↓
<i>Haemophilus sp. HMT 908</i>	Exposure (hpe)	-0.33869	0.101631	1.23 x 10-03	2.16 x 10-02	0.712701	28.73	↓
<i>Neisseria cinerea</i>	Exposure (hpe)	-0.28912	0.087623	1.37 x 10-03	2.16 x 10-02	0.748926	25.11	↓
Unclassified <i>Fretibacterium</i>	Macrophages/mg	-0.00196	0.000538	4.53 x 10-04	8.95 x 10-03	0.998045	0.20	↓
<i>Prevotella intermedia</i>	Macrophages/mg	-0.00155	0.000501	2.63 x 10-03	3.32 x 10-02	0.998452	0.15	↓
<i>Treponema sp. HMT 237</i>	Macrophages/mg	-0.00139	0.000416	1.16 x 10-03	1.83 x 10-02	0.998609	0.14	↓
<i>Cattonella morbi</i>	Macrophages/mg	-0.00098	0.000266	3.70 x 10-04	8.95 x 10-03	0.99902	0.10	↓
Unclassified <i>Neisseriaceae</i>	Macrophages/mg	-0.00086	0.000286	3.36 x 10-03	3.32 x 10-02	0.99914	0.09	↓
<i>Selenomonas sp. HMT 478</i>	Macrophages/mg	-0.00083	0.000274	3.18 x 10-03	3.32 x 10-02	0.999169	0.08	↓
<i>Alloprevotella sp. HMT 473</i>	Macrophages/mg	0.001429	0.000299	6.37 x 10-06	2.52 x 10-04	1.00143	0.14	↑
<i>Porphyromonas sp. HMT 278</i>	Macrophages/mg	0.001812	0.000362	2.52 x 10-06	1.99 x 10-04	1.001814	0.18	↑
<i>Stomatobaculum longum</i>	Age	0.178938	0.040569	7.57 x 10-05	2.99 x 10-03	1.195946	19.59	↑
<i>Alloprevotella sp. HMT 308</i>	Age	0.190333	0.040621	3.21 x 10-05	2.53 x 10-03	1.209652	20.97	↑
Unclassified <i>Selenomonas</i>	Exposure (hpe)	0.231395	0.072505	1.93 x 10-03	2.53 x 10-02	1.260357	26.04	↑
<i>Alloprevotella sp. HMT 473</i>	Sex (Male)	1.822075	0.541339	1.69 x 10-03	4.46 x 10-02	6.184676	518.47	↑

Supplementary Table E13. Negative Binomial Mixed Model Results for Genus-Level Microbiome Differential Abundance Analysis Using SILVA

	Estimate	Std.Error	p-value	p-adj	Exp.Estimate	Percent Change	Increase/Decrease
<i>Fretibacterium</i>	-0.442817	0.0872207	1.65 x 10-06	6.60 x 10-05	0.642224723	35.78	↓
<i>Campylobacter</i>	-0.4147313	0.115686	5.11 x 10-04	1.02 x 10-02	0.660517738	33.95	↓
<i>Leptotrichia</i>	-0.197746	0.0677126	4.27 x 10-03	4.27 x 10-02	0.820578254	17.94	↓
<i>Selenomonas</i>	0.1751485	0.0553511	2.03 x 10-03	2.71 x 10-02	1.19142313	19.14	↑

Supplementary Table E14. Negative Binomial Mixed Model Results for Species-Level Microbiome Differential Abundance Analysis Using SILVA

	Estimate	Std.Error	p-value	p-adj	Exp.Estimate	Percent Change	Increase/Decrease
<i>Campylobacter cunicolorum</i>	-0.4147313	0.11568601	5.11 x 10-04	0.012014716	0.660517738	33.95	↓
Unidentified Leptotrichia	-0.3683424	0.08195423	1.79 x 10-05	0.000839771	0.691880241	30.81	↓
Unidentified Selenomonas	0.1751485	0.05535112	2.03 x 10-03	0.031787511	1.19142313	19.14	↑

Supplementary Table E15. Negative Binomial Mixed Model Results for Genus-Level Host-Microbiome Association Analysis Using SILVA

	Variable	Estimate	Std.Error	p-value	p-adj	Exp.Estimate	Percent Change	Increase/Decrease
<i>Fretibacterium</i>	Exposure(hpe)	-0.55138	0.088516	1.31 x 1008	5.24 x 1007	0.576152	42.38	↓
<i>Campylobacter</i>	Exposure(hpe)	-0.52979	0.141547	3.13 x 1004	6.26 x 1003	0.588728	41.13	↓
<i>Fretibacterium</i>	Macrophages per mg	-0.0016	0.000421	2.60 x 1004	5.21 x 1003	0.998402	0.16	↓
<i>Catonella</i>	Macrophages per mg	-0.00097	0.00025	2.02 x 1004	5.21 x 1003	0.999033	0.10	↓
Unclassified Burkholderiales	Exposure(hpe)	0.294879	0.093209	2.10 x 1003	2.80 x 1002	1.342964	34.30	↑

Supplementary Table E16. Negative Binomial Mixed Model Results Species-Level Host-Microbiome Association Analysis Using SILVA

	Variable	Estimate	Std.Error	p-value	p-adj	Exp.Estimate	Percent Change	Increase/Decrease
<i>Campylobacter cunicolorum</i>	Exposure (hpe)	-0.52979	0.141547	0.000313	0.014718	0.588728	41.13	↓
Corynebacterium unidentified	Exposure (hpe)	-0.29927	0.096419	0.002524	0.029657	0.741362	25.86	↓
Leptotrichia unidentified	Exposure (hpe)	-0.29654	0.094433	0.002257	0.029657	0.743388	25.66	↓
Catonella unidentified	Macrophages per mg	-0.00097	0.00025	0.000202	0.009478	0.999033	0.10	↓
Unclassified Burkholderiales	Exposure (hpe)	0.294879	0.093209	0.002099	0.029657	1.342964	34.30	↑

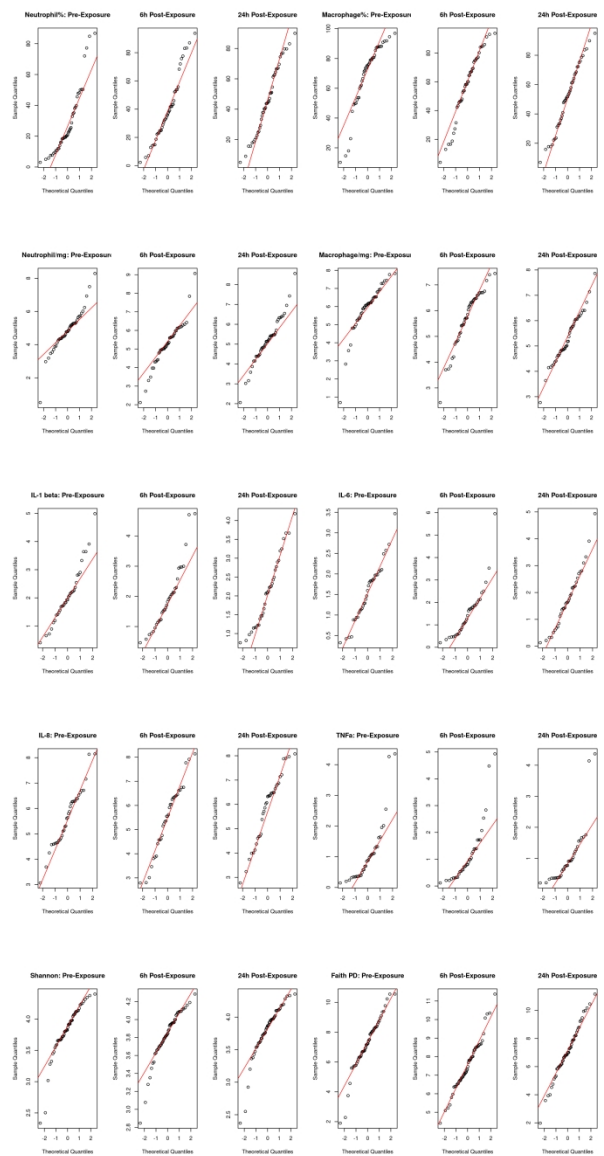


Figure E1

645x1291mm (118 x 118 DPI)

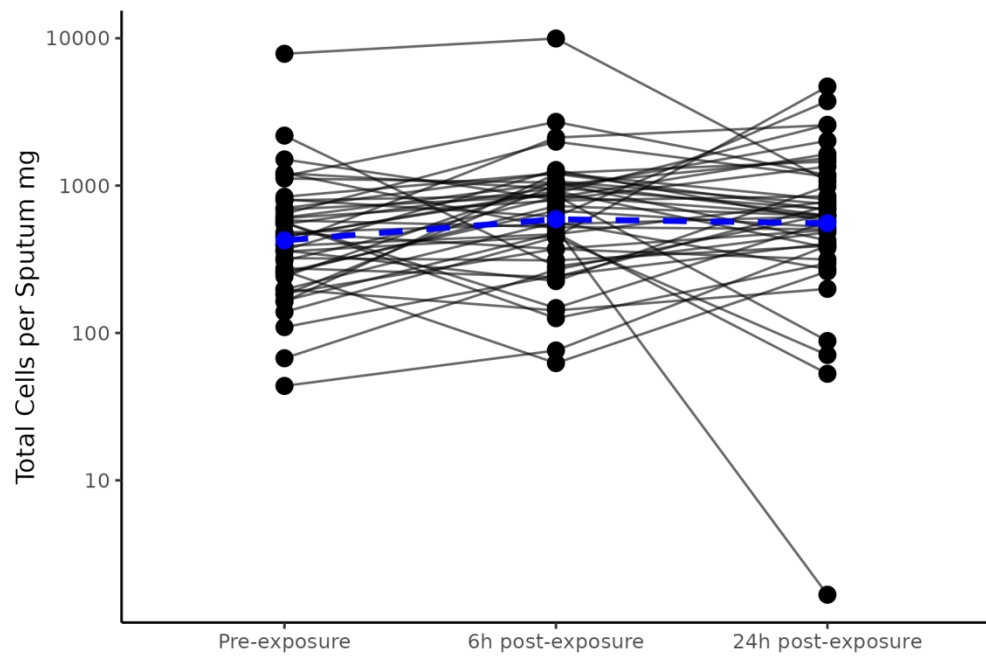


Figure E2

387x258mm (118 x 118 DPI)

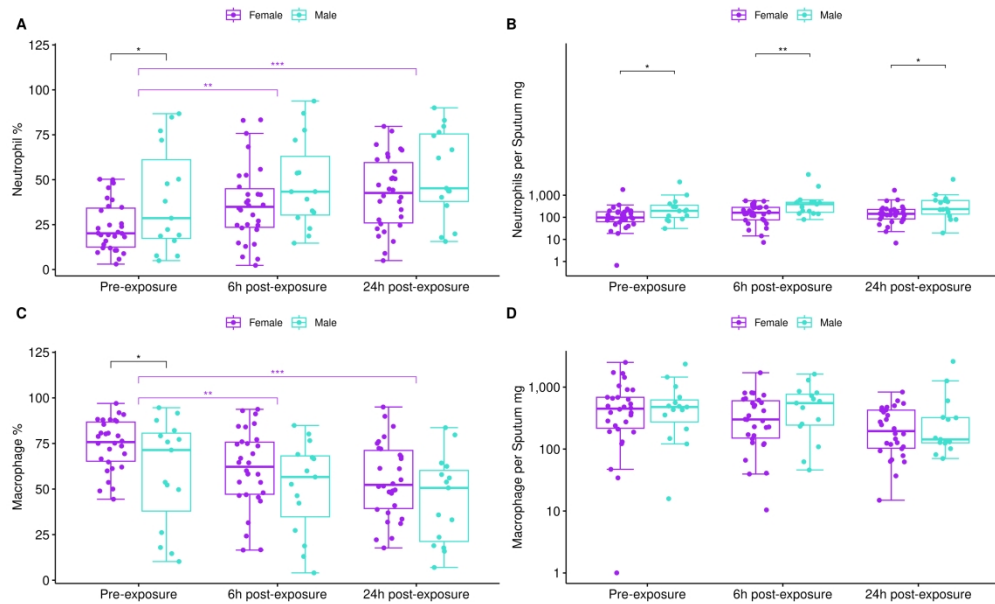


Figure E3

839x516mm (118 x 118 DPI)

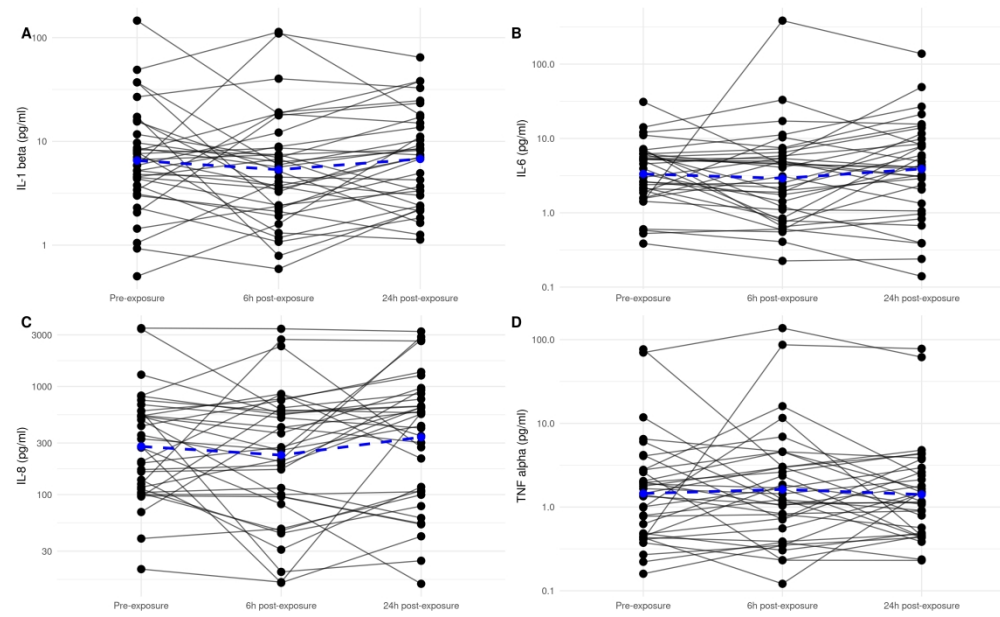


Figure E4

839x516mm (118 x 118 DPI)

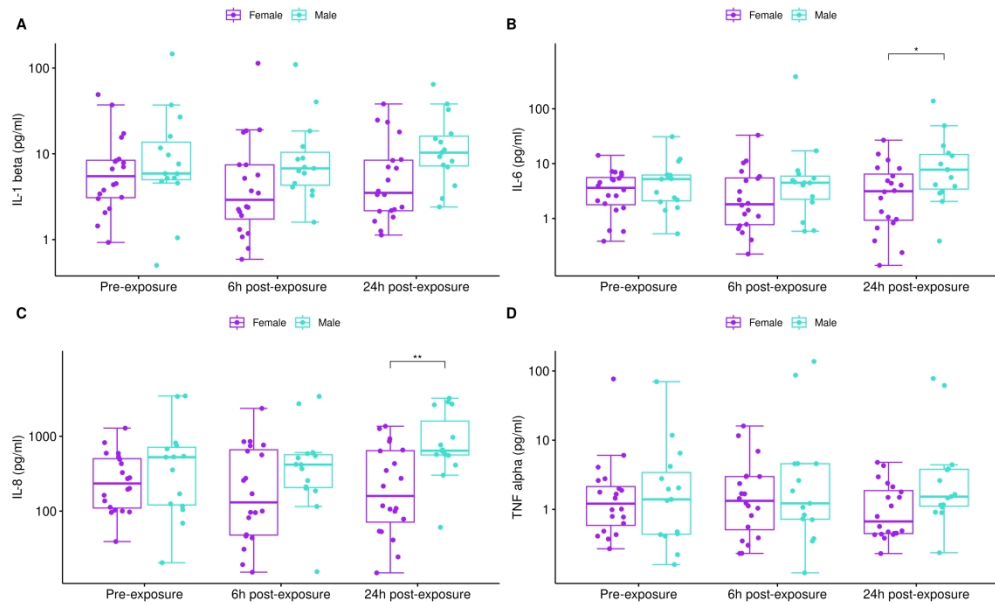


Figure E5

839x516mm (118 x 118 DPI)

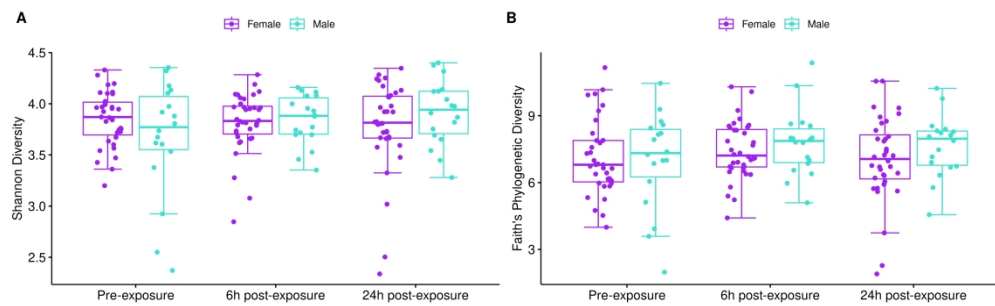


Figure E6

839x258mm (118 x 118 DPI)

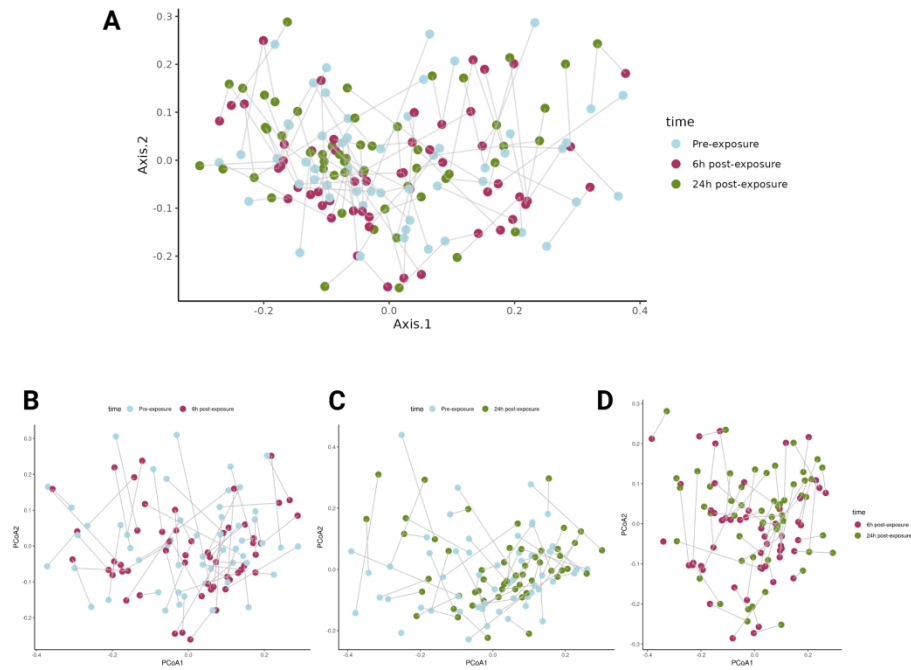


Figure E7

536x450mm (118 x 118 DPI)

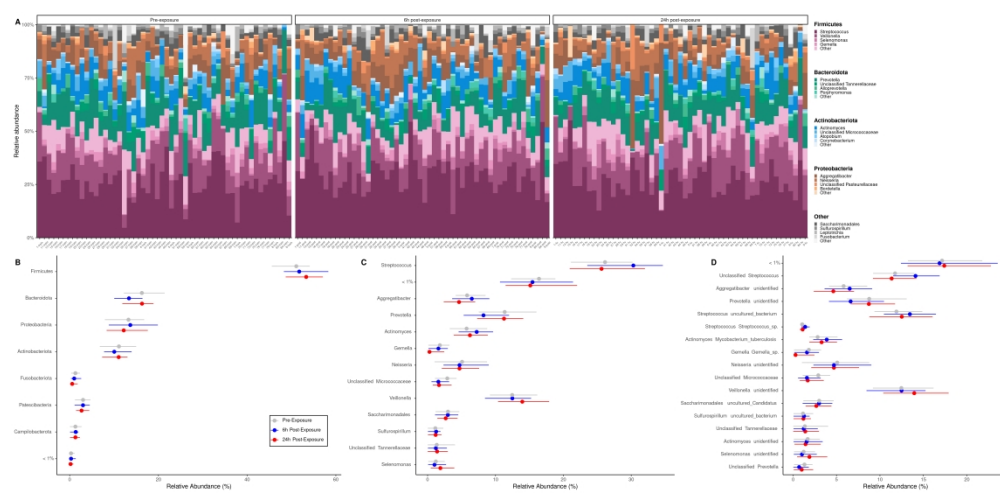


Figure E8

1614x774mm (118 x 118 DPI)

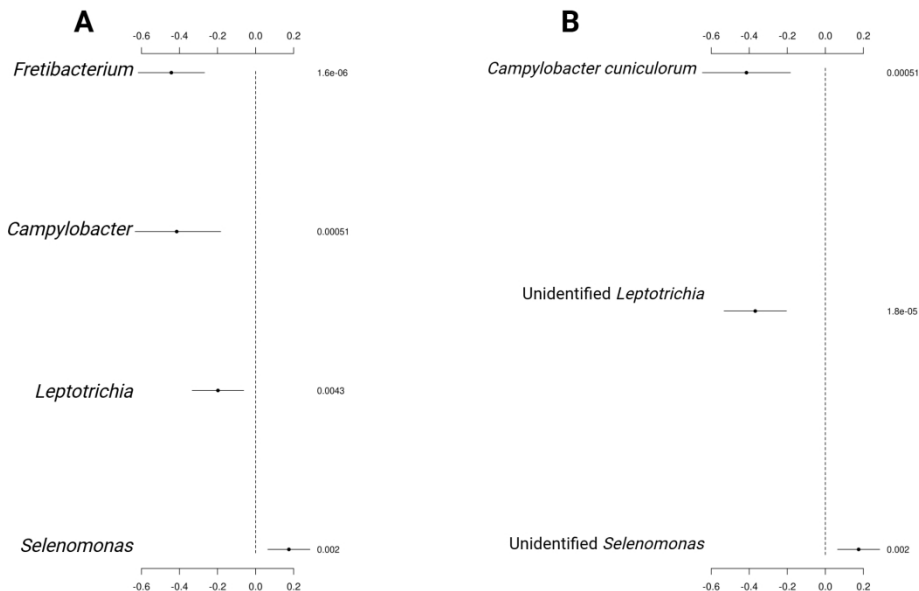


Figure E9

481x362mm (118 x 118 DPI)

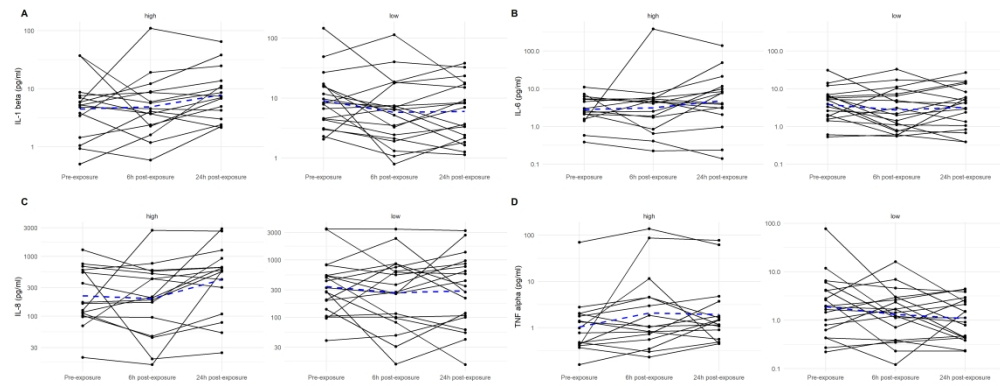


Figure E10

1291x516mm (118 x 118 DPI)